Ancient TL

www.ancienttl.org · ISSN: 2693-0935

Issue 9(3) - November 1991
https://doi.org/10.26034/la.atl.v9.i3

Improved detection of EPR signals used in quartz dating

W. Jack Rink† and Yuhei Shimoyama‡
†Subdepartment of Quaternary Research, University of Cambridge, Free School Lane, Cambridge, CB2 3RS, England.
‡Department of Physical Chemistry, University of Cambridge, Lensfield Road, Cambridge, CB2 1EW, England.

Vector electron paramagnetic resonance spectroscopy has been successfully applied to the quartz phase of granites and rhyolites. The E' centre signal has been selectively detected by complete suppression of the OHC signal, thereby resulting in a well defined isolated spectrum for spin concentration determination. This is achieved by variation of the phase of the magnetic field modulation, and takes advantage of saturation transfer which occurs during the relaxation process of the E' centre.

Introduction

EPR dating (usually referred to as ESR dating) has found wide application in Quaternary geochronology and archaeometry (Grün, 1989) and more recently has shown potential for dating back to the Precambrian using quartz (Odom et al, 1989). EPR dating of quartz is presently in a development stage, with efforts underway to date volcanic, plutonic and hydrothermal crystallization of quartz as well as to date faults, cementation in sandstone and ancient heating of flint. The physical basis of EPR dating has been reviewed by Grün (Grün, 1989).

Two types of radiation-induced defect centres which are important to dating quartz are the E' centre (Grün, 1989) and the so called OHC (peroxy radical) centre (Rink and Odom, 1991). The E' centre signal has primarily been used in efforts to date faults (Fukuchi et al, 1986; Ikeya et al, 1982). The E' centre signal, which may be due to one or more types of similar defects, involves oxygen vacancies containing unpaired electrons (Yip and Fowler, 1975; Weil, 1984). In fused silica, two different types of OHC centres are attributed to trapped holes on non-bridging peroxy sites (Friebele et al, 1979). Similar paramagnetic defects apparently occur in crystalline quartz, evidenced by the similarity of the OHC signals in fused quartz to certain signals in crystalline quartz. The precise nature of the OHC centres in quartz is still a source of controversy (Rink and Odom, 1991).

The E' centre in quartz is usually detected by using a microwave power level between 0.01 and 0.1 (mW) (Odom et al, 1989). However, this procedure may only partially suppress the OHC signal. Complete suppression of the OHC signal is important to dating quartz with EPR because in some cases it interferes with determination of the signal intensity of the E' centre. The primary aim of this paper is to describe how improved selective detection of the E' signal can be achieved by the Vector EPR Method.

The Vector EPR Method has been developed firstly in the systems of nitroxide radicals in solution (Shimoyama and Watari, 1986) and later applied to other paramagnetic species (Shimoyama et al, 1990,Watari et al, 1989). The non-linear response of electron spins under saturating conditions is found to be useful, because it promotes a drastic phase change. This phase change then allows the detection of a signal component whose phase shift away from the in-phase position depends upon the relaxation rate of the electron spins (Shimoyama and Watari, 1985).

Experimental Methods

The quartz was separated from the granites using standard methods described elsewhere (Rink and Odom, 1991), and from the rhyolite using H_2SiF_6 acid treatment of the <50 μm fraction to remove feldspars. EPR measurements have been made using a JEOL X-band spectrometer (RE-1X). All spectra were observed with the first harmonic absorption mode (first derivative display), and modulated/demodulated at 100 kHz/100kHz frequencies. The sample was placed at the centre of the cylindrical cavity (TE_{011} mode) in an unsealed fused quartz sample tube.

The phase of magnetic field modulation was varied over the entire available 360° range at intervals of 30°. Two important phase positions of field modulation were identified in the present study: the null phase (also termed out-of-phase or quadrature) and the in-phase of filed modulation. In order to determine these specific values of field modulation, first the OHC signal was observed using 10 mW microwave power and arbitrary phase of field modulation. Then the phase was adjusted to obtain zero intensity of the OHC signal, which is defined as the null phase (Shimoyama and Watari, 1989). At the null phase position, only the E' centre signal was obtained. Then the in-phase value was obtained by simply adjusting the phase of field modulation to a position 90° away from the null phase position.

Results

Figure 1 shows the results of variation between the null phase and the in-phase of field modulation on the spectrum of quartz from the Libyan Addaba Mohamed Salah granite (El-Makhrouf, 1988). fig. 1A shows the in-phase OHC signal, extending from $g \approx 2.010$ to 2.003. In contrast, the spectrum when measured under null phase conditions (fig. 1B) shows only the E' centre at $g \approx 2.001$. Importantly, note also that the OHC signal is completely suppressed. Selective detection of the E' signal has therefore been achieved. Less complete suppression of the OHC signal can be achieved using a microwave power level ca. 0.1 mW or less, as shown in fig. 1C. Selective detection of the E' centre was also achieved using quartz from the Overflow Pond Granite (Dallmeyer et al, 1983) from Newfoundland. Figs. 1D and 1E show similar results obtained for quartz from the Castell Grug Intrusive Rhyolite (Fitch, 1967) from North Wales.

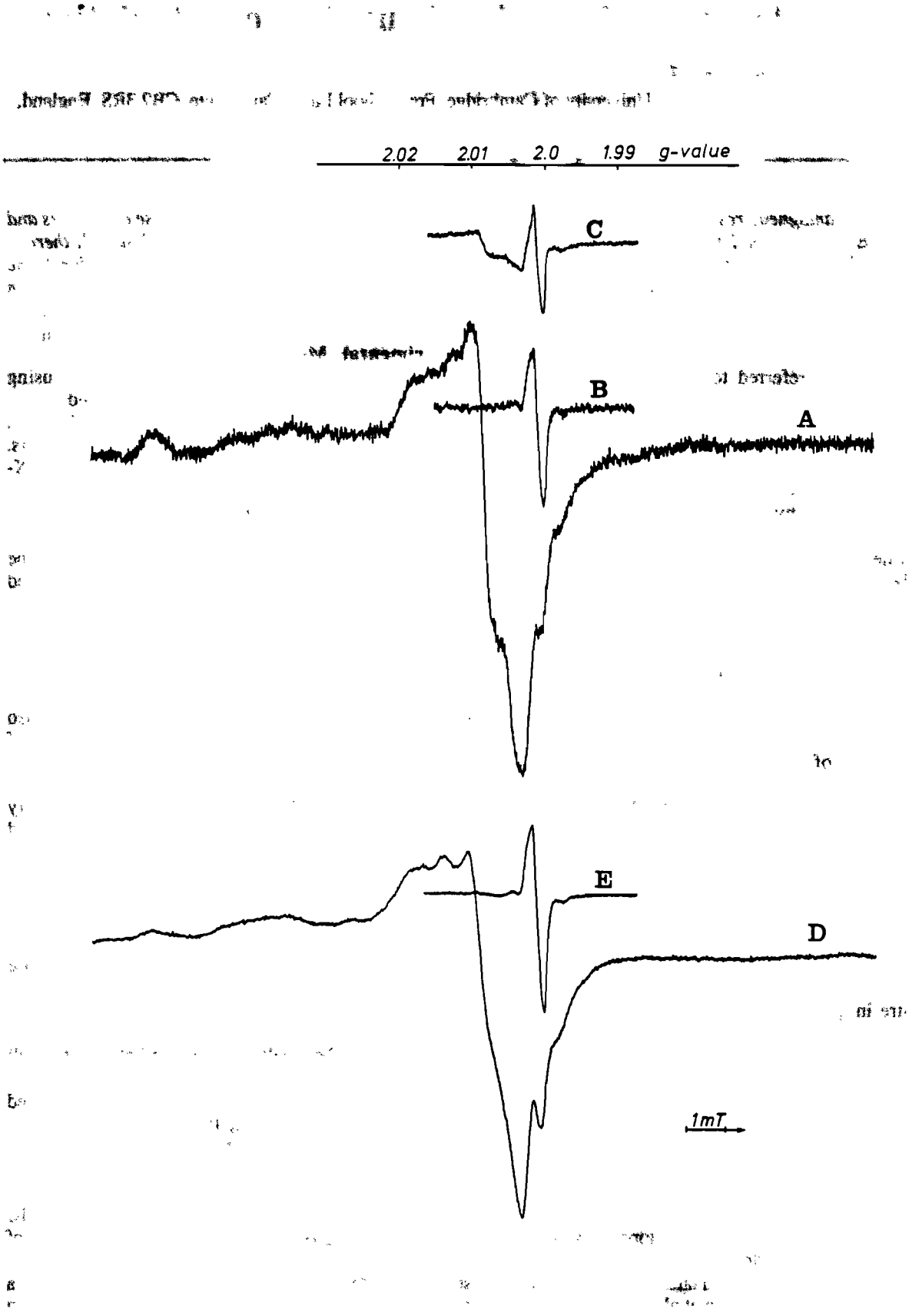

Figure 1. EPR spectrum of quartz isolated from the Addaba Mohamed Salah granite (A, B, C) and Castell Crug intrusive rhyolite (D,E) under various experimental conditions. A and D) in-phase spectrum showing OHC signal between g ≈ 2.010 and 2.003 obtained at 10 mW microwave power. B and E) null phase spectrum showing only E' centre signal obtained at 10 mW power. C) in-phase spectrum showing E' signal and OHC signal obtained at 0.1 mW power. All spectra obtained using 0.2 mT modulation amplitude.

Figure 2 shows the variation of the peak-to-peak amplitude of the first harmonic absorption of the E' and OHC signals as a function of the phase of field modulation. It is seen in fig. 2B that at 0.05 mW microwave power, where little saturation is involved, both the E' and OHC signals behave similarly. This clearly shows that neither signal can be selectively detected using this approach. On the other hand, fig. 2A shows that at 10 mW microwave power, a phase offset appears, which displaces the E' centre about 90° away from the OHC signal. Trow at 90° in fig. 2A indicates the null phase position used to record the spectrum in fig. 1B, whereas the arrow at 0° indicates the in-phase position for obtaining the spectra of fig. 1A and 1C.

Discussion

Previous attempts at selective detection of the E' signal obtained only the type of spectrum shown in fig. 1C, in which the OHC signal may still be a significant component of the spectrum. Complete suppression of the OHC signal yields the E' signal on a flat baseline (fig. 1B). This is extremely useful when integration of the E' signal is employed in spin concentration determinations. E' centre spin concentration determinations are used in the development of a quartz dating method that involves Schottky-Frenkel radiation defects (Rink and Odom, 1991; Rink, 1990).

The saturation transfer phenomenon that promotes signal suppression during quadrature detection can be induced by two different mechanisms. They are spectral diffusion and saturation recovery (Shimoyama and Watari, 1986). Since the quartz system involves only hindered molecular motion, spectral diffusion is not expected. Therefore, saturation recovery is mainly responsible for saturation transfer in the quartz system. The process of saturation recovery depends upon the relaxation times of the various paramagnetic species in the quartz. The saturation transfer due to the saturation recovery modulates the inherent phase of the resonance line with respect to the reference wave of field modulation. The other words, the passage or velocity of field change associated with 100 kHz field modulation at certain applied fields detects phase differences due to different relaxation times of the OHC and E' centres in the quartz.

It is clear that application of this technique will have considerable value in selective detection of signals embedded within complex spectra of other minerals suitable for EPR dating. This is because microwave power saturation is often used to remove undesirable signals in minerals used for dating.

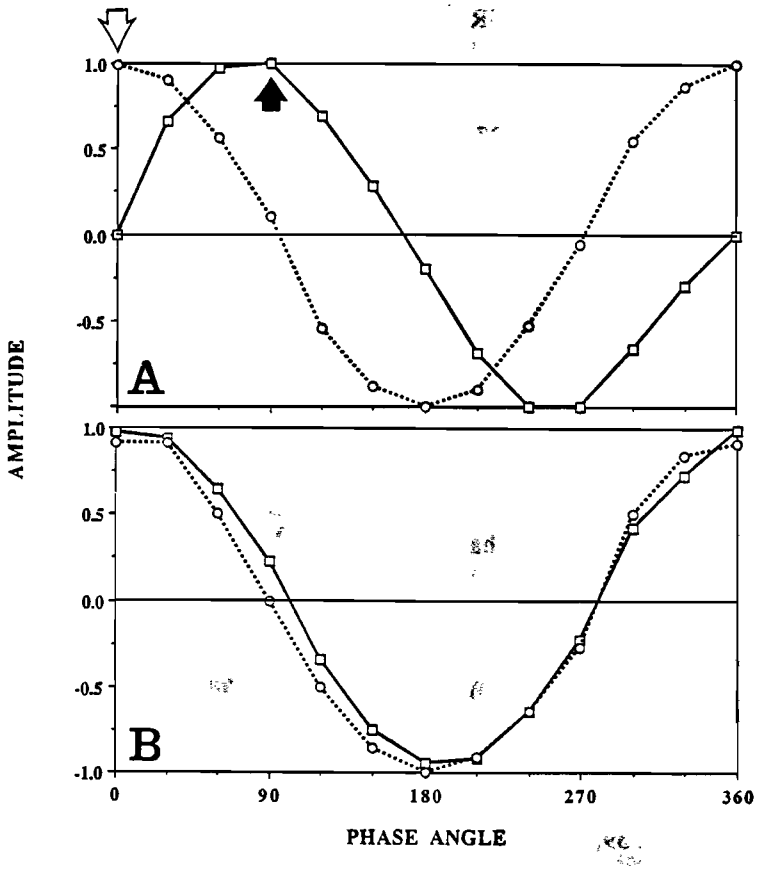

Figure 2. Variation of normalized peak-to-peak amplitudes of the first harmonic absorption of the E' (squares) and OHC (circles) signals versus phase of magnetic field modulation. A) 10 mW microwave power, B) 0.05 mW microwave power. The arrows indicate the null phase position (dark arrow) and the in-phase position (open arrow) used to obtain the spectra of figs. 1B and 1A respectively.

Acknowledgements

W.J.R. and Y.S. thank Dr. R. Grün for his helpful review of the manuscript. Y.S. thanks Dr. Ray Freeman for his courtesy. Y.S. also acknowledges the Royal Society of London as well as the Japan Society for Promotion of Sciences for their help. This material is based upon work supported by the North Atlantic Treaty Organization under a grant awarded to WJR. in 1990. W.J.R. also thanks Dr. A. L. Odom for his continuing support.

References

Dallmeyer, R. D., Odom, A. L. and Kean, B. F. (1983) Age and contact-metamorphic effects of the Overflow Pond granite: an undeformed pluton in the Dunnage Zone of the Newfoundland Appalachians, *Can. J. Earth Sci.* **20**, 1639-1645.

El-Makhrouf, A. A. (1988) Tectonic interpretation of Jabal Eghei area and its regional application to the Tibesti orogenic belt, South Central Libya (S.P.L.A.J.), *J. African Earth Sci.* **7**, 945-967.

Fitch, F. J. (1967) Ignimbrite Volcanism in North Wales, *Bull. Volcanology* **30**, 199-219.

Friebele, D. L., Griscom, D. L., Stapelbroek, M., and Weeks, R. A. (1979) Fundamental defect centres in glass: the peroxy radical in irradiated, high purity silica, *Phys. Rev. Lett.* **42**, 1346-1349.

Fukuchi, T., Imai, N. and Shimokawa, K. (1986) ESR dating of fault movement using various defect centres in quartz; the case in the western South Fossa Magna, Japan, *EPSL* **78**, 121-128.

Grün, R. (1989) Electron spin resonance (ESR) dating, *Quat. Int.* **1**, 65-109.

Ikeya, M., Miki, T. and Tanaka, K. (1982) Dating of a fault by ESR of intrafault materials, *Science* **215**, 1392-1393.

Odom, A. L. and Rink, W. J. (1989) Natural accumulation of Schottky-Frenkel defects: Implications for a quartz geochronometer, *Geology* **17**, 55-58.

Rink, W. J. (1990) Experimental and theoretical investigation of radiation-induced point defects in quartz: implications for geochronometry, unpublished Ph.D Thesis, Florida State University, Tallahassee, Florida, USA.

Rink, W. J., and Odom, A. L. (1991) Natural alpha recoil particle radiation and ionizing radiation sensitivities in quartz detected with EPR: Implications for geochronometry, *Nuclear Tracks and Radiat. Measts* **18**, 163-173

Shimoyama, Y., Ichikawa, O. and Watari, H. (1990) Vector saturation transfer ESR studies of coal, *Fuel* **69**, 1237-1242.

Shimoyama, Y. and Watari, H. (1985) Phase behaviours of saturation transfer ESR signals at high microwave fields, *Appl. Spectrosc.* **39**, 170-173.

Shimoyama, Y. and Watari, H. (1986) Analysis of saturation transfer electron paramagnetic resonance spectra in terms of amplitude and phase, *J. Chem. Phys.* **84**, 3688-3695.

Shimoyama, Y. and Watari, H. (1989) Multiple harmonic electron paramagnetic resonance spectroscopy by simultaneous detection, *Appl. Spectrosc.* **43**, 1021-1026.

Weil, J. A. (1984) A review of electron spin spectroscopy and its application to the study of paramagnetic defects in crystalline quartz, *Phys. Chem. Min.* **10**, 149-165.

Watari, H., Murakami, M., Seo, Y. and Shimoyama, Y. (1989) Vector electron paramagnetic resonance spectroscopy with first and second harmonic display of ferrihemoglobin, *Biochem. Biophys. Res. Commun.* **162**, 681-685.

Yip, K. L. and Fowler, W. B. (1975) Electronic structure of E'_1 centres in SiO_2, *Phys. Rev. B* **B11**, 2327-2338

PR Reviewed by S.W.S. McKeever

The effect of optical absorption on luminescence dating

A.G. Wintle and G.A.T. Duller
Institute of Earth Studies, University College of Wales, Aberystwyth, SY23 3DB. UK

Introduction

Knowledge of the thermoluminescence emission spectra of minerals has led to the choice of particular optical filters when trying to enhance the response of a particular mineral relative to another. This approach has been used particularly for fine grained sediments, which cannot be separated by mineralogical techniques (Debenham and Walton, 1983). Although emission spectra for some samples of quartz and feldspar are now available (Huntley et al, 1988), no parallel studies of the optical absorption properties of the minerals have been published. In this paper we discuss the importance of such properties for luminescence dating studies.

Published absorption data for feldspars

Most absorption spectra result from electronic transitions relating to the presence of elements such as iron and manganese in the crystals. These result in characteristic absorption bands in the visible and near infrared region and relate to the colour of the crystal (Rossman, 1988). Electronic transitions between the top of the valence band and the bottom of the conduction band will result in absorption in the W, as well as the production of a luminescence signal as a result of ionization. Spectral measurements indicate absorption in the near UV at wavelengths of less than 320 nm.

Hofmeister and Rossman (1983) consider this absorption to be caused by charge transfer from oxygen to a cation (probably Fe^{3+}). It is characterized by a very steeply rising absorption edge. In their review Hofmeister and Rossman gave several examples of feldspars exhibiting this response (orthoclase, labradorite and amazonite). Figure la reproduces their graph of data from Speit and Lehmann (1976) for a sanidine from the Eifel area of Germany, where the effect of heating the crystal results in the shift of the apparent absorption edge from about 380 nm back to 320 nm. Comparison of these spectra with the absorption spectra of X-ray irradiated crystals shows that irradiated grains have an intense absorption band at about 360 nm.

Effects of absorption in the near UV

i) Because of the need for quartz optics to observe the near UV and because of the difficulty in calibrating the spectrometer response below 350 nm, most emission spectra are only obtained for wavelengths greater than 350 nm. For example, Huntley et al (1988) demonstrated that K feldspar TL is dominated by emission around 400 nm (fig. lb). However, it is possible that the peak at 400 nm is caused by the effect of absorption on an emission peak further into the UV. If selective absorption is occurring, then the relative spectra will differ if the measurements are made on grains of different sizes; less absorption will occur for the signal from fine grain samples than for the <1 mm crushed grains used by Huntley et al. The spectrum will also be affected by past radiation or heat treatments.

ii) A more direct effect of optical absorption may be expected when luminescence dating is carried out using an optical filter which spans the absorption edge, e.g. the Schott UGll whose transmission characteristics are shown in figure lc. The UGll has been used alone and in combination with heat absorbing filters (e.g. Chance-Pilkington HA-3) which restrict its transmission to wavelengths greater than 280 nm. For fine grain sediments, no difference in the EDs obtained using either blue or UV filters have been reported. However, problems with apparent underestimation of ED have been reported when the luminescence of coarse-grained K feldspars has been observed with a UGll filter (Balescu et al, 1991; Dijkmans and Wintle, 1991). Detailed examination of the response of a particular Danish feldspar by Grün et al (1989) suggested that a higher ED was obtained when using a predominantly blue transmitting filter combination (Corning 7-59 and HA3) and they suggested that this could be related to a more stable luminescence signal. More recently Balescu and Lamothe (1991) demonstrated a consistent difference between EDs obtained with ultraviolet filters (Schott UGll or Hoya U340) and with a blue filter (Corning 7-59) for K feldspars from beach deposits in northwest Europe. On the other hand, no difference was observed by the same authors for K feldspars from southern Italy. The magnitude of the discrepancy in the ED values was found to be equivalent to that which would be calculated as being due to the internal dose rate within K feldspar grains - about 40% for the grains in the above study.

The grains involved in the study were relatively coarse (150 - 250 or 250 - 300 μm) and so if the etched grains were effectively only emitting UV light from the surface because of strong absorption, then the ED obtained would relate to that surface layer. The dose to this layer due to the internal potassium of the grain will be smaller than the average to the whole grain.

Comparing the absorption spectrum of natural smoky sanidine (fig la) and the filter combinations that have been used in the dating of potassium feldspars (fig lc) it is clear that the TL signal observed with the UG11 filter (with or without a heat-absorbing filter) will be absorbed within the crystal. Even with the 7-59 filter

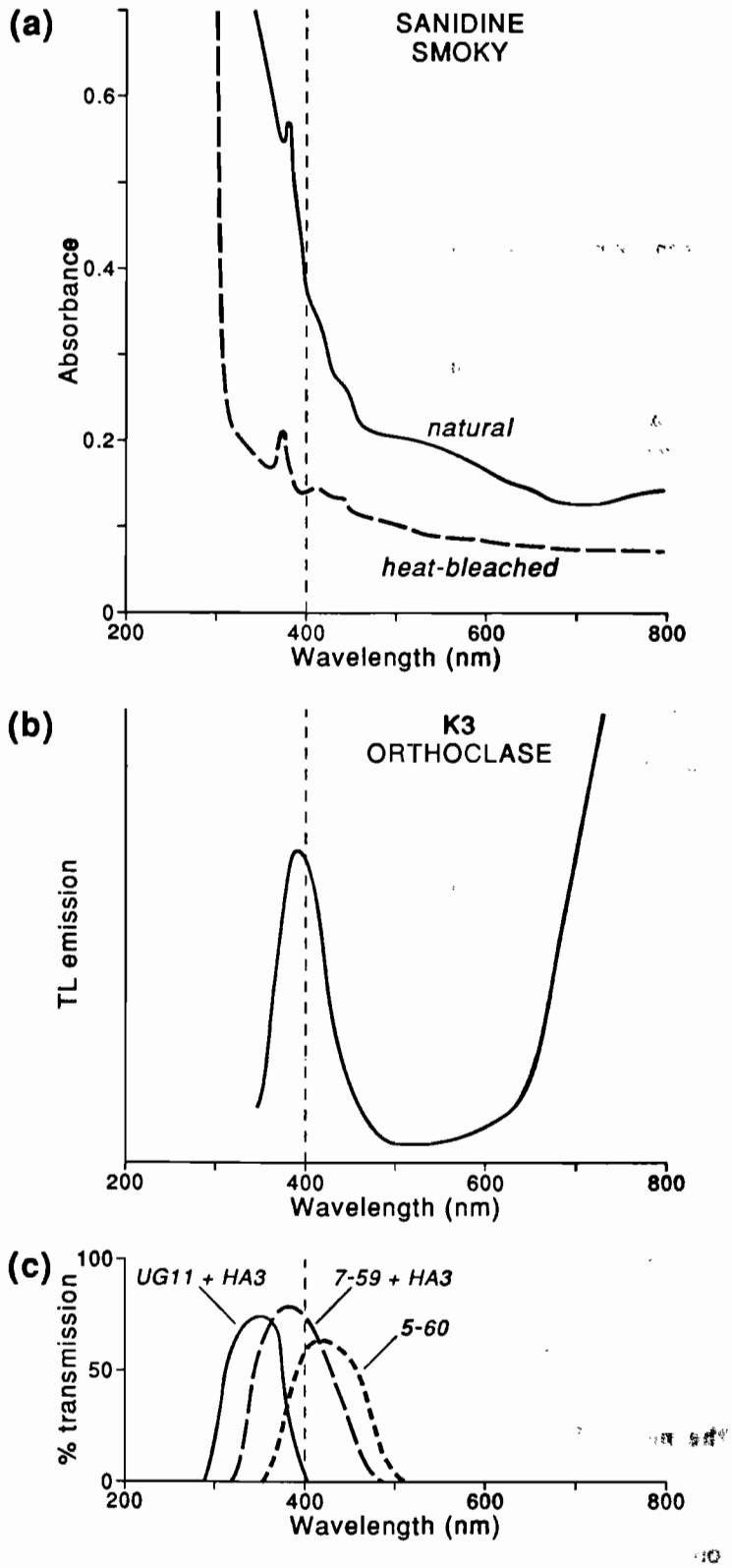

Figure 1. (a) Absorption spectra for smoky sanidine taken from Hofmeister and Rossman (1983); (b) emission spectrum for potassium feldspar (K3 orthoclase) from Huntley et al (1988); c) transmission characteristics of filters commonly used in TL dating studies. The vertical dashed line at 400 nm indicates the wavelength below which absorption is likely to affect luminescence measurements.

some absorption is likely and this was suggested by the results presented by Grün et al (1989). However, Mejdahl's use of a Corning 5-60 filter (Kolstrup et al, 1990) would result in little absorption of the signal from 300 μm grains. This is demonstrated by the agreement between the ages that he obtains for quartz and feldspar separates from the same sample.

Obviously different feldspars will show individual absorption characteristics and some examples are given by Hofmeister and Rossman (1983). The absorption properties of individual feldspar grains used in dating studies could be studied with a microscope uv-visible spectrophotometer, but the exact position of the absorption edge also depends upon crystal orientation. A simpler solution is to use filters which transmit above 400 nm.

References

Balescu, S. and Lamothe, M. (1991) The blue emission of K-feldspar coarse grains and its potential for overcoming TL age underestimation. *Quaternary Science Reviews*. in press.

Balescu, S., Packman, S.C. and Wintle, A.G. (1991) Chronological separation of interglacial raised beaches from Northwestern Europe using thermoluminescence. *Quaternary Research* **35**, 91-102.

Debenham, N.C. and Walton, A.J. (1983) TL properties of some wind-blown sediments. *PACT* **9**, 531-538.

Dijkmans, J.W.A. and Wintle, A.G. (1991) Methodological problems in thermoluminescence dating of Weichselian cover sand and Late Holocene drift sand from the Lutterzand area, E. Netherlands. *Geologie en Mijnbouw* **70**, 21-33.

Grün, R., Packman, S.C. and Pye, K. (1989) Problems involved in TL-dating of Danish cover sands using K-feldspar. Synopses from *Workshop on Long and Short Range Limits in Luminescence Dating*. Occasional paper 9 of the Research Laboratory for Archaeology, Oxford.

Hofmeister, A.M. and Rossman, G.R. (1983) Color in feldspars. *Reviews in Mineralogy* **2**, 271-280.

Huntley, D.J., Godfrey-Smith, D.I., Thewalt, M.L.W. and Berger, G.W. (1988) Thermoluminescence spectra of some mineral samples relevant to thermoluminescence dating. *Journal of Luminescence* **39**, 123-136.

Kolstrup, E., Grun, R. Mejdahl, V., Packman, S.C. and Wintle, A.G. (1990) Stratigraphy and thermoluminescence dating of Late-Glacial cover sands in Denmark. *Journal of Quaternary Science* **5**, 207-224.

Rossman, G.R. (1988) Optical Spectroscopy. *Reviews in Mineralogy* **18**, 207- 243.

Speit, B. and Lehmann, G. (1976) Hole centers in the feldspar sanidine. *Physica Status Solidi* **36A**, 471-481.

PI Reviewer's Comments (Helen Rendell)

The absorption of UV TL emissions by feldspars, as discussed in this paper, represents at least a partial explanation of the age underestimates obtained from large grain potassium feldspars. The dosimetry implications are likely to be strongly dependent on grain size. Other explanations of underestimation relating to long-term signal instability or the methods used for the calculation of the new internal beta dose distribution still need to be explored more fully.

On the selection of dose points for saturating exponential ESR/TL dose response curves

Rainer Grün and Edward J. Rhodes
Subdept. of Quaternary Research, Cambridge University, Free School Lane, Cambridge CB2 3RS, UK.

Introduction

During the past few years, it has been suggested that linear extrapolation of the ESR/TL dose response may not be an appropriate procedure for determining the equivalent dose, D_E, when using the additional dose method (Apers et al., 1981; Berger et al., 1987; Poljakov and Hütt, 1990; Grün and Macdonald, 1989). In this paper we have performed numerical simulations of exponential dose response curves using random numbers which are more fashionably called Monte Carlo simulations. We wanted to investigate the influence of the applied dose distribution, the precision of the ESR/TL intensity measurement, and the number of data points on error in the D_E determination.

Franklin (1986) examined this question of optimization for linear fitting and concluded that, from a mathematical point of view, the minimum error in D_E determination might be attained from repeated measurements of the lowest and highest dose points. He suggested that the measurement of a dose point in the middle may be used to demonstrate linearity of the dose response. This may be directly applicable to single exponential fitting, when the dose response is converted into a straight line by fitting $-\ln(1 - I/I_{max})$ versus the artificial dose, where I is the measured ESR signal intensity and I_{max} is the maximum ESR signal intensity when all traps are filled (Apers et al., 1981).

Barabas (1989) carried out some Monte-Carlo simulations on saturating exponential functions and came to the conclusion that at least 12-15 measurements with a maximum gamma irradiation dose, $D_{\gamma(max)}$, of 1500 Gy ought to be carried out in order to achieve an error in D_E determination of about 10% for a D_E of 500 Gy and where the characteristic saturation dose, D_0, (see figure 1) is about 1500 Gy. However, as far as we are aware, no systematic numerical simulations have been carried out in order to determine the influence of the number of measurements and the placing of the radiation dose steps on the uncertainty in D_E determination. In many ESR or TL dating studies, the number of dose points and their placing seems very random.

Experimental Procedures

The basic assumptions and procedures for our computational experiments are as follows: the dose response is described by a single saturation function of the type: $I = I_{max} \{1 - \exp(-(D_\gamma + D_E)/D_0)\}$ where D_γ is the additional artificial gamma dose and D_0 is defined in figure 1. In order to reduce computation time, the data points were converted into a straight line function by rearranging the above equation so that we could plot $-\ln(1 - I/I_{max})$ versus $(D_\gamma + D_E)/D_0$. The iteration process followed the following procedure: after inserting an initial value for I_{max} into the above equation, D_0 and D_E are readily calculated by applying the method of least squares (LSQ) to the straight line (see eg Berger and Huntley, 1986). I_{max} was then iteratively optimized using the method of least squares to the original saturating exponential function and the whole process was repeated until changes in I_{max} were smaller than 0.1%. All data points were given the same precision. Although this straight line conversion may not always give the best fit when compared to a three parameter optimizing procedure (see Grün and Macdonald, 1989), the differences of the calculated values compared to the latter approach (where I_{max}, D_0, and D_E are optimized at the same time) are usually smaller than 1% for all determined parameters. We used a random number generator to create a Gaussian distribution with a preset precision around a given mean value. The model assumes that the uncertainty in the dose can be neglected (see also Berger and Huntley, 1986; Berger et al., 1987).

Our calculations are based on a typical experimental ESR dose response curve of the paramagnetic centre at g=2.0018 of tooth enamel with D_0 = 3333 Gy. Since the results are generally valid for any I_{max} value and D_E/D_0 ratio, we also give the latter value.

Three basic different dose distributions were investigated:

model 1: even dose spacing, (e.g. 0, 2, 4, 6, 8 ....);

model 2: doubling of an initial dose step (e.g. 0, 1, 2, 4, 8....);

model 3: exponential dose distributions $[D_\gamma = 10 \{\exp(bN) - 1\}]$, where b is a constant (in the range 0.1 to 0.9) and N ranges from 0 to 9.

We have performed our simulations for various preset D_E values of 10, 50, 100, 500, 1000 and 5000 Gy (which correspond to D_E/D_0 ratios of 0.003, 0.015, 0.03, 0.15, 0.3 and 1.5, respectively). The basic computational procedure was as follows: first a saturating exponential function was defined by selecting preset values for D_0 and I_{max} followed by the

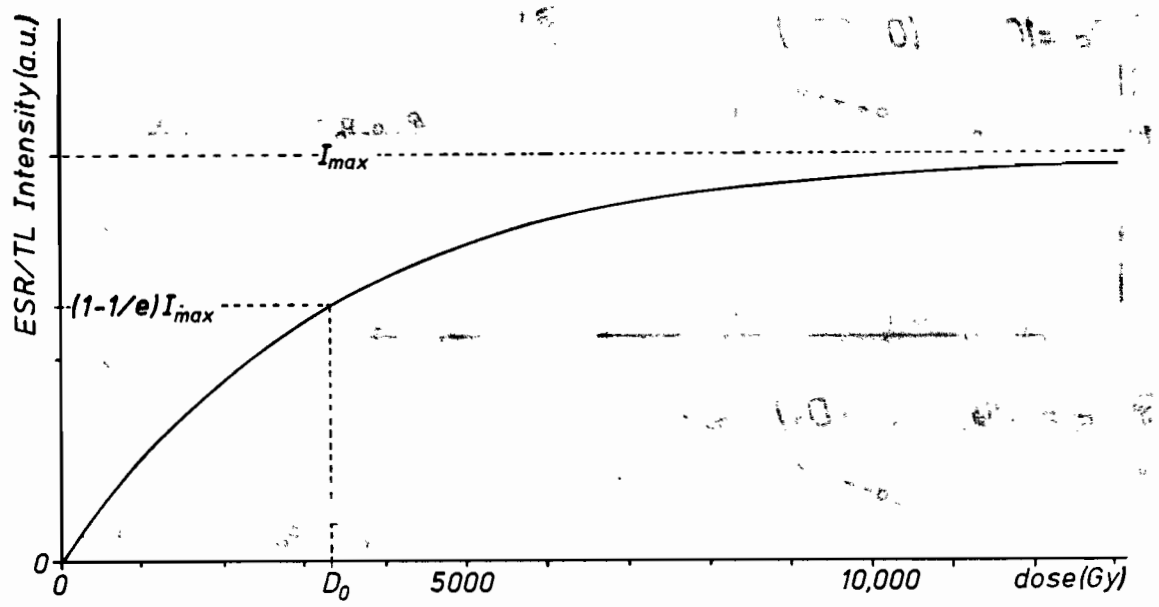

Figure 1. The dose response curve that was used in the computer simulation. I: measured ESR/TL intensity; I_{max}: maximum intensity when all traps are filled; D_0: characteristic saturation dose.

selection of the preset D_E and the number of different dose points. Then, the precision of the intensity measurements was defined and a dose distribution model with a particular D_{max} value was chosen. The random number generator then produced successively 1000 sets of ESR/TL intensity values within the preset precision. These sets were used to determine 1000 D_E values.

We have checked the mean and the standard deviation of the randomly produced intensities and observed that the mean of the generated intensities differed less than 0.1% from the intensity values of the defined function, and the standard deviation showed variations in the range of 5% from the preset value. The computations were carried out on a computer with a 25 MHz 80486 CPU. The program was written in Microsoft Quick Basic.

Results

Effect of the maximum irradiation dose, $D_{\gamma(max)}$.

In the first experiment, the precision (1σ - standard deviation) of each ESR/TL intensity is 2% (which is probably smaller than in most routine dating analyses) and 10 data points per dose response curve were used (most ESR dating results are based on fewer points).

Figures 2a and 2b show the standard deviation (s.d.) in the determination of D_E, and the systematic deviation of the computed mean D_E value from the preset D_E. The exponential dose step models 2 and 3 result in smaller errors than the even dose distribution (model 1). Additionally, the minimum error for models 2 and 3 is far less dependent on the applied maximum dose, $D_{\gamma(max)}$, than model 1.

In the D_E range from 10 to 1000 Gy (0.003 to 0.3 D_0), the optimum $D_{\gamma(max)}$ value for model 1 is about 4 to 6 times D_E, whereas the optimum $D_{\gamma(max)}$ value for models 2 and 3 is about 10 times D_E. For the optimum $D_{\gamma(max)}$, the s.d. of the D_E determination is in the 5-7% range. Above 1000 Gy ($0.3D_0$), the calculated error becomes more critically dependent on the selection of $D_{\gamma(max)}$ and an D_E determination of 1.5 D_0 has a s.d. in the range of at least 25%. This error rapidly increases with a change in $D_{\gamma(max)}$. Figure 2b seems to imply that $D_{\gamma(max)}$ should not exceed about 3 times D_0 when $D_E \geq D_0$.

In the D_E range 10 to 100 Gy (0.003 to 0.03 D_0), a low $D_{\gamma(max)}$ value seems to lead to a systematic underestimation in D_E. However, if $D_{\gamma(max)} > 5$ times D_E, this underestimation is less than 3%. In the D_E range of 500 to 1000 Gy (0.15 to 0.3 D_0), high $D_{\gamma(max)}$ values lead to systematic overestimation of D_E. Again, if $D_{\gamma(max)}$ is 10 times D_E or smaller, the overestimation is below 3%. D_E estimations in the 5000 Gy (1.5 D_0) range seem to be associated with severe overestimation (>15%).

The determination of I_{max} is also strongly dependent on the choice of $D_{\gamma(max)}$: a close approximation to the preset values of I_{max} and D_0 is possible only when $D_{\gamma(max)}$ is in the range of D_0. However, the correct estimation of I_{max} and D_0 do not necessarily influence the precision and accuracy of the D_E determination. The D_E determinations with the smallest uncertainties in the low dose range (10 to 100 Gy or 0.003 to 0.03 D_0) may be associated with errors of many hundred percent in the determination of I_{max} and D_0.

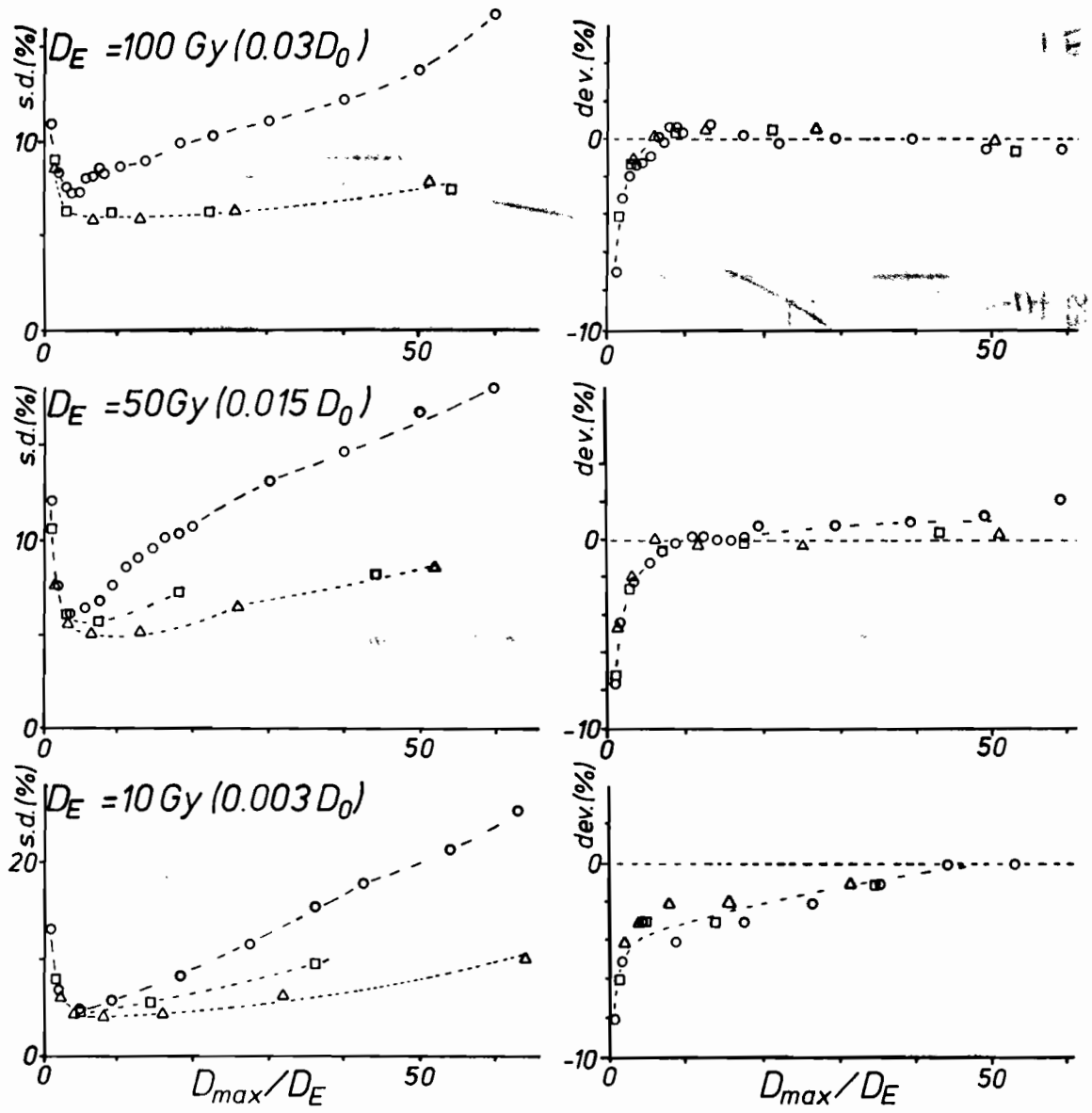

Figure 2a. Standard deviation, s.d., (left) and systematic deviations (right) in DE determination for preset D_E values of 10, 50 and 100 Gy (0.003, 0.015 and 0.03 D_0), and a precision in ESR/TL intensity of 2%. Dose spacing according model 1 (circles), model 2 (triangles) and model 3 (squares).

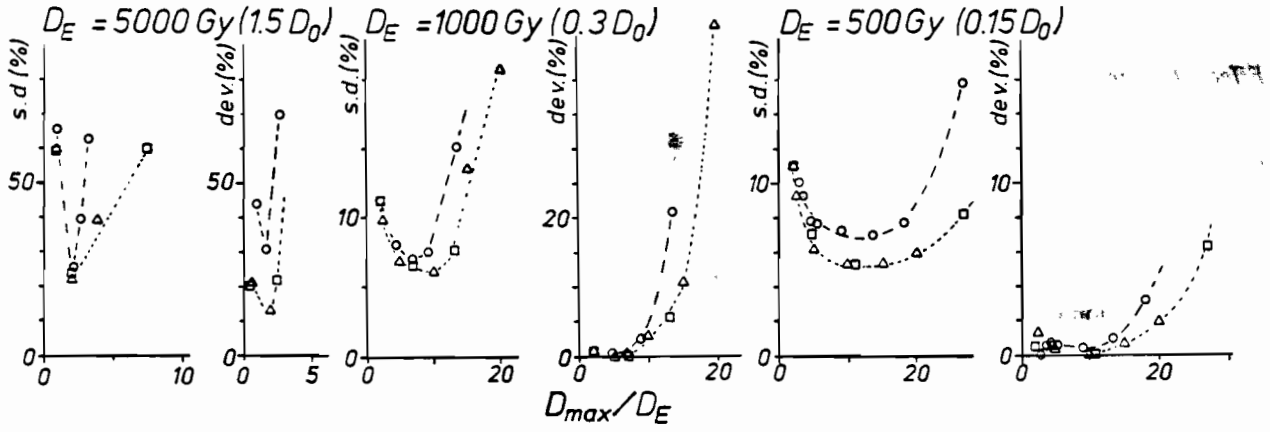

Figure 2b. Standard deviation, s.d., (left) and systematic deviations (right) in D_E determination for preset D_E values of 500, 1000 and 5000 Gy (0.15, 0.3 and 1.5 D_0), and a precision in ESR/TL intensity of 2%. Dose spacing according model 1 (circles), model 2 (triangles) and model 3 (squares).

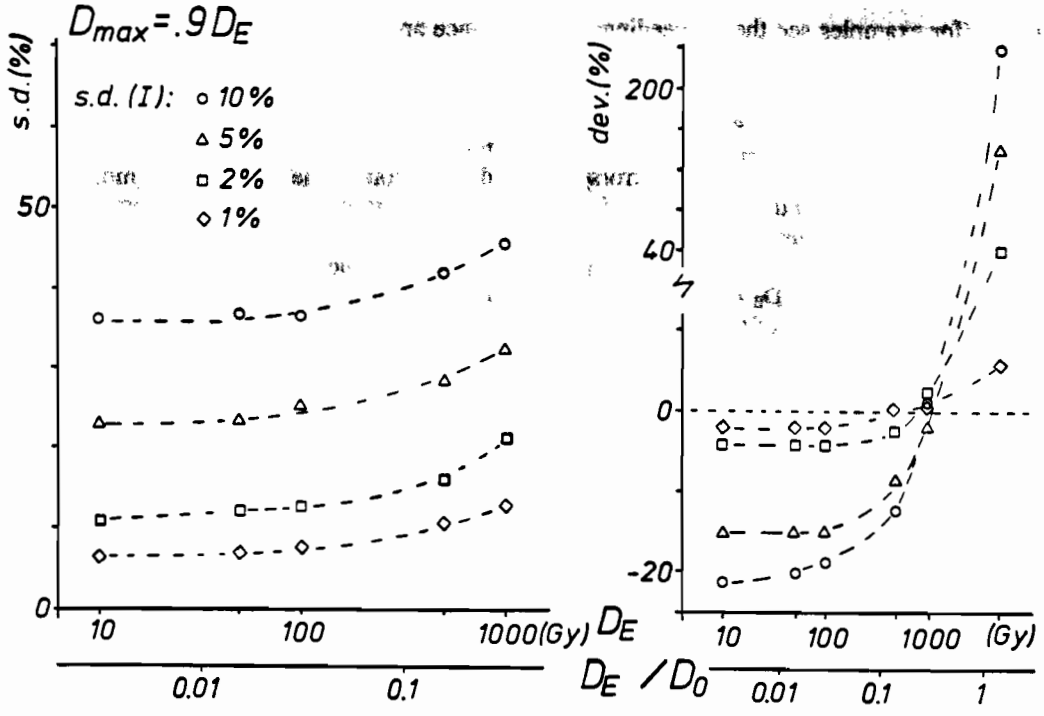

Figure 3. Standard deviation, s.d., (left) and systematic deviations (right) in D_E determination for $D_c(max)$ = 0.9 D_E using model 1. X-axis: preset D_E.

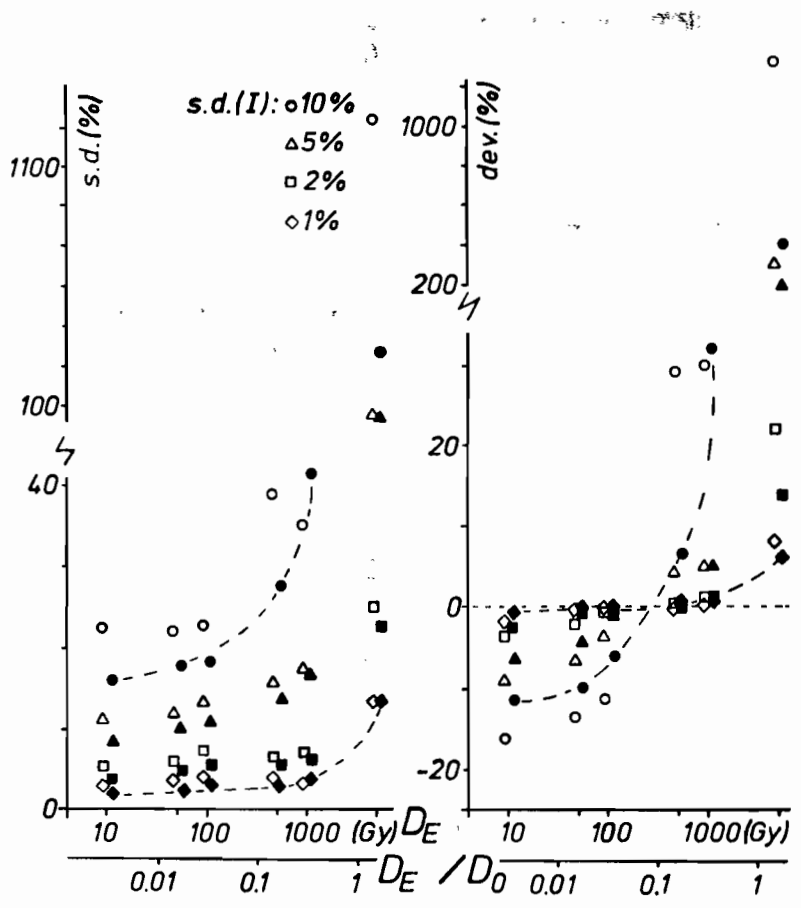

Figure 4. Standard deviation, s.d., (left) and systematic deviations (right) in D_E for different precisions in ESR/TL intensity and optimum $D_c(max)$ according Figure 2. Open symbols: dose spacing model 1; closed symbols: dose spacing model 2. X-axis: preset D_E.

Some publications (for examples see the Proceedings of the TL/ESR seminars in *Quaternary Science Reviews* vol. 7 (1988) or *Nuclear Tracks and Radiation Measurements* vols 10(1985), 14(1988) and 18(1991)) show dose response curves where $D_{\gamma(max)}$ is smaller than the determined D_E value. Figure 3 shows the errors that are involved in these cases (10 dose points). This selection causes a s.d. in D_E of at least 10% (with the same conditions as for the above simulation). Both the s.d. and the systematic deviation in D_E determination increase rapidly with lower precision of the data points (see also figures 4 and 5).

Effect of the precision of the ESR/TL intensity.
Figure 4 shows the D_E estimations for different precisions of the generated ESR/TL intensities (10 dose points, model 1, $D_{\gamma(max)}$ selected to produce minimum errors in D_E). For the s.d. in D_E to be smaller than 10%, the precision of the measured ESR/TL intensities must be better than 5% (in the D_E range of 10 to 1000 Gy [0.003 to 0.3 D_0]). A precision of 1% still causes a s.d. of > 10% for an D_E determination of 5000 Gy (1.5 D_0). Simulations with precisions of 5% and less are also associated with large systematic underestimations (10 to 100 Gy [0.003 to 0.03 D_0]) and over-estimations (>500 Gy [0.15 D_0]).

Effect of the number of dose points.
Figure 5 shows that the error in the D_E determination cannot be significantly improved by additional measurements within the same dose range. In all cases, an D_E determination from 10 dose points with a 1% precision has a smaller s.d. and a smaller systematic deviation in D_E than from 40 dose points with a 2% precision. In the D_E range of 10 to 1000 Gy (0.003 to 0.3 D_0), D_E estimations based on 4 different dose points with a precision of 1% lead to better results than D_E estimations derived from 40 different dose points with a precision of 2%. This result parallels for exponential fitting the predictions of Franklin (1986) for linear fitting. It therefore seems advisable to put any spare energy into decreasing the uncertainty of the measured ESR/TL intensities (see also Berger and Huntley, 1989).

Discussion

Our simulation shows that significant deviations in D_E determination occur only at relatively small $D_{\gamma(max)}/D_E$ ratios (<3-5) where all dose points are relatively closely spaced or when the ESR/TL intensities have low precision and are dependent on the computational procedures that we have selected for our calculations: the largest possible D_E for a given data set is determined by a linear function (i.e. I_{max} approaches infinity). While this determines the maximum possible D_E, there is basically no restriction for the determination of the minimum possible D_E and the resulting D_E values do not show a Gaussian distribution around the mean value. As soon as the curvature of the dose response curve is strong enough that no fitting effectively results in a straight line, the D_E distribution becomes symmetrical.

Since an exponential distribution of dose steps is less affected by the correct selection of $D_{\gamma(max)}$ and leads to slightly smaller errors in D_E than equally spaced dose distribution, it seems to be optimal to select a suitable maximum irradiation dose and to use an exponential distribution of the dose points (models 2 and 3). Our simulations show that any effort in minimizing the error in the D_E determination ought to go into minimizing the deviation of the ESR/TL measurement by repeated measurements at one dose, rather than measuring additional dose points. Figure 5 implies that 4 dose points with a 1% precision in the ESR/TL intensity lead to better results than 40 different dose points with 2% precision (the former can be achieved by measuring 4 different dose points with 4 aliquots with 2% precision resulting in a 1% standard error of the mean). However, we do not generally recommend the measurement of three or four additional dose steps only, because it will not allow the recognition of systematic deviations from the assumed mathematical model of the dose response curve. Additionally, see Berger's comments for restrictions in TL.

Our simulations suggest that in order to assess the errors that are involved in the D_E estimation, it is necessary to estimate the precision of a routine ESR/TL measurement (see also Berger and Huntley 1989). This precision may vary strongly from mineral to mineral and is generally larger in TL than in ESR (partly because the latter technique can measure much larger samples). Berger and Huntley (1986, 1989) and Berger et al (1987) point out that the intrinsic error of a TL measurement is not known. Little is known about the intrinsic error of an ESR measurement; repeated measurements of ESR intensities of speleothems varied between 2-5% (Grün, 1985), the reproducibility of the measurement of the OHC and E' centres in quartz are in the range of 1.5% (Rhodes, unpublished data) and the precision of ESR measurements in mollusc shells was assumed to be in the range of 3% (Barabas, 1989).

One way of estimating the precision of intensity measurements of a particular material is to calculate the scatter of the data points around the regression line for a large number of similar samples. ESR measurements of tooth enamel lie normally within less than 1% around the exponential regression line (using both equal weights and weights inverse proportional to the square of the intensity) and ESR measurements of corals lie in the range of 1 to 2% around the regression line (Grün, unpublished data).

We wish to emphasize that the reported results are valid only if the ESR/TL dose response curve is precisely described by a single saturation function. In cases where this assumption is violated, for example by supralinearity, the occurrence of several overlaying saturation functions (Katzenberger and Willems, 1988), trap production (Grün, 1990; Berger, 1990), or occurrence of a "dose pit" (see Shlukov and Shakhovets, 1987; Grün, 1991), all errors and deviations that result from applying an incorrect mathematical function are much larger.

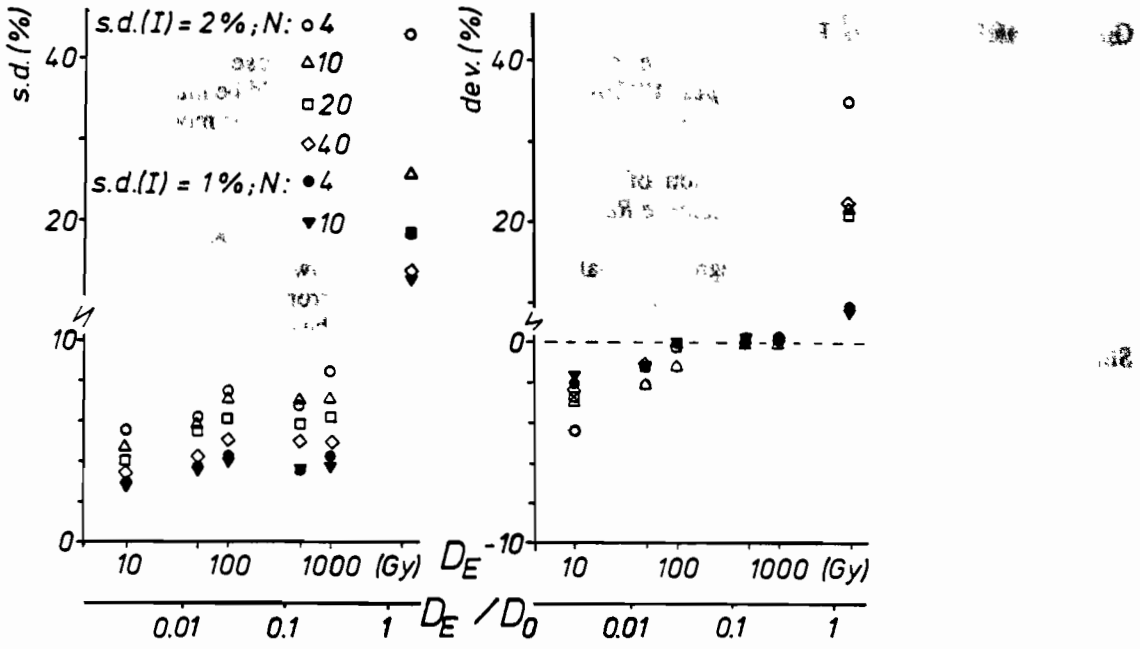

Figure 5. Standard deviation, s.d., (left) and systematic deviations (right) in D_E determination for different number of data points, N, and optimum D_c(max) according Figure 2 using dose spacing model 1. X-axis: preset D_E.

Initial simulations using weights of the ESR/TL intensity that are proportional to the ESR/TL intensity (as suggested by Berger and Huntley, 1989) show that the results reported above are qualitatively correct, however, this approach leads to smaller overall errors. These results will be reported in a forthcoming paper.

Conclusion

The size of the D_E error in our simulation is critically dependent on the precision of the measured ESR/TL intensity. Additionally, the uncertainty in the D_E estimation is dependent on the selected $D_{\gamma(max)}$ and the dose step distribution. This suggests that the samples should be monitored before irradiation in order to estimate the approximate D_E. Additional effort should go into increasing the precision of the data points. Measurements of less than 7 dose points can be recommended only if the dose response curve is known to follow a single saturation function.

The curve fitting procedure used in this paper is routinely applied in our laboratory; however, without further systematic simulations, the results cannot directly be generalized for other fitting procedures (e.g. using different weighting of the data points: see Berger and Huntley, 1986 and 1989; Berger et al., 1987) and methods of error assessment.

Acknowledgements

This study was partly funded by a NERC research fellowship to E. Rhodes and a SERC grant to N. J. Shackleton. We thank the referee for many helpful suggestions.

References

Apers, D., Debuyst, R., DeCanniere, P., Dejehet, F. and Lombard, E. (1981) A criticism of the dating by electron paramagnetic resonance (ESR) of the stalagmitic floors of the Caune de l'Arago at Tautavel. In: DeLumley, H. and Labeyrie, J. (eds) *Absolute dating and isotope analysis in prehistory - methods and limits.* Preprint, S. 533-550.

Barabas, M. (1989) ESR-Datierung von Karbonaten: Grundlagen, Systematic, Anwendungen. Inaugural Dissertation, Universität Heidelberg, 161 p.

Berger, G.W. (1990) Regression and error analysis for a saturating-exponential-plus-linear model. *Ancient TL* **8**, 23-25.

Berger, G.W., and Huntley, D.J. (1986) Linear regression of TL data. *Ancient TL* **4**, 26-29.

Berger, G.W., and Huntley, D.J. (1989) Test data for exponential fits. *Ancient TL* **7**, 43-46.

Berger, G.W., Lockhart, R.A., and Kuo, J. (1987) Regression and error analysis applied to the dose-response curve in thermoluminescence dating. *Nuclear Tracks and Radiation Meas.* **13**, 177-184.

Franklin, A.D. (1986) Extrapolation errors in linear regression. *Ancient TL* **4**, 31-35.

Grün, R. (1985) Beiträge zur ESR-Datierung. Sonderveröffentlichungen des Geologischen Instituts der Universität zu Köln, **59**, 1-157.

Grün, R. (1990) Dose response of the paramagnetic centre at g = 2.0007 in corals. *Ancient TL* **8(3)**, 20-22.

Grün, R. (1991) Potential and problems of ESR dating. *Nuclear Tracks and Radiat. Meas.* **18**, 143- 153

Grün, R., and Macdonald, P.D.M. (1989) Non-linear fitting of TL/ESR dose response curves. *Applied Radiation and Isotopes* **40(10-12)**, 1077-1080.

Katzenberger, O., and Willems, N. (1988) Interferences encountered in the determination of AD of mollusc samples. *Quaternary Science Reviews*, **7(3/4)**, 485- 489.

Poljakov, V., and Hütt, G. (1990) Regression analysis of exponential palaeodose growth curves. *Ancient TL* **8**, 1-2.

Shlukov, A.I., and Shakhovets, S.A. (1987) Kinetic studies of quartz thermoluminescence as applied to sediment dating. *Ancient TL* **5(1)**, 11-15.

PR Reviewer's Comment (Glenn Berger)
This is a welcome addition to the published discussions on error analysis in TL/ESR dating studies. Monte Carlo simulations can provide powerful discrimination among the effects of the various inputs (assumptions and parameters) to regression and error models. Hopefully, such simulations will continue to be carried out in this area. However, as the authors point out, there are limitations to the conclusions one can draw from this first such detailed simulations in TL/ESR studies.

The assumption of equal weights to all data points (rather than weighting by inverse variance such as in Berger et al., 1987) may invalidate the author's conclusion for situations where the extrapolation from the range of artificial doses is relatively large (e.g., $D_e/D_0 > 0.1$ here, or relative extrapolations of >40% in the terminology of Berger et al., 1987). It would be instructive to test this possible invalidation by simulations with models that use unequal weighting.

The authors' results also re-emphasize the importance of acquiring a firmer knowledge of the "intrinsic" variance or precision in each measurement of TL/ESR intensity. As discussed elsewhere (Berger et al., 1987; Berger and Huntley, 1989), there may be serious difficulties with attempting to measure reliably this variance for TL signals. However, it seems likely that the intrinsic variance of ESR signals can be measured reliably, though different values may be needed for each type of material. In this context ESR has an advantage over TL because signal intensities can be replicated on the same subsample, thus factoring out the disc-to-disc and related effects associated with replication of TL signals. Therefore, if reliable estimates of intrinsic variance in ESR signals can be obtained, then it would be straightforward to apply a Chi-squared goodness-of-fit test routinely to ESR growth curve data, and thereby provide an objective criterion for the recognition of spurious (outlier) data points (see e.g., Brooks et al., 1972). Of course, application of such a test depends for its validity on our confidence in the particular regression model that we choose (e.g., Berger 1990).

There is a further point to note. Although the authors qualify their results as applicable only to their curve-fitting procedure, their discussion of the effects of the number of dose points (second paragraph in Discussion) could be misinterpreted as relevant to other "procedures" (error models), which it is not. That is, their model shows that increasing the number of data points at one dose point has a greater effect than if the same increase were distributed among several dose points. In contrast, equations 4 and 10 of Berger et al. (1987) show that with that error model (constant percent error, weighting inversely proportional to variance) the error in D_E can be reduced by *any* increase in the number of data points, without regard to how these data points are distributed among the chosen dose points, or whether new dose points are added. Of course, the low-dose (low TL intensity) data points have greater weight in this error reduction. The distinction of this behaviour from that of the authors' procedure may lie in their operational definition of precision. These comments are meant to draw further attention to the continued need for comparison of different error analysis models using common data sets (eg Berger and Huntley, 1989).

The above additional comments thus re-emphasize the importance of "model awareness" when interpreting computed regression errors, and the importance of acquiring a firmer knowledge of "intrinsic" TL/ESR errors, as discussed above.

Brooks, C., Hart, S.R. and Wendt, I. (1972) Realistic use of two-error regression trestments as applied to rubidium-strontium data. *Rev. Geophys. Space Phys.* **10**, 5510577.

The bleaching of latent optically stimulated luminescence

R. B. Galloway
Department of Physics, University of Edinburgh, Mayfield Road, Edinburgh, EH9 3JZ, Scotland.

Introduction

The very nature of optically stimulated luminescence (OSL) ensures that samples are liable to bleaching by even short exposure to laboratory illumination during preparation. The results are reported here of tests on quartz and feldspar samples exposed to 1200 mm long 40 W fluorescent tubes at a distance of 1 m. Three colours of fluorescent light were investigated, red which has a long history of use in the preparation of samples for thermoluminescence measurement, gold which was the subject of a recent report in relation to thermoluminescence (Galloway and Napier, 1991) and white which served to indicate the extent of any benefit from the use of coloured light. The red tube emits a continuous distribution of wavelengths from 600-800 nm peaked at 640 nm and provides 20 mW m^{-2} at a distance of 1 m, the gold tube emits a continuous distribution of wavelengths from 510-750 nm peaked at 580 nm and provides 100 mW m^{-2} at a distance of 1 m, while the white tube emits over the wavelength range 310-720 nm with emission lines particularly noticeable at 610, 550, 440, 405 and 360 nm and provides 500 mW m^{-2}, Thorn EMI Lighting (1987). Fine grain samples of quartz were prepared from 'acid washed sand' (BDH Ltd., Broom Road, Poole BH12 4NN, England) and fine grain felspar samples from Norwegian microcline material. They were drained of natural luminescence either by heating to 500 °C or by exposure in a SOL-2 solar simulator for 30 minutes. Each sample was exposed to a $^{90}Sr/^{90}Y$ beta source to provide a radiation dose of 240 Gy and then pre-heated at 200 °C for 60 s to empty thermally unstable traps. An OSL measurement of 1s duration (which released less than 1% of the latent signal) was made on each sample for normalisation prior to exposure of the sample to light. Similarly normalised samples were measured without light exposure for reference before each sequence of exposures while samples were stored in the dark for the duration of the sequence and measured subsequently to ensure that no fading occurred which was unrelated to light exposure.

For the infra red stimulated luminescence of feldspar the LED system described by Galloway (1991) was used, providing an estimated 50 mW cm^{-2} at the sample and with luminescence detection being by EMI 9635QA photomultiplier preceded by 2 mm Schott BG 39, 4 mm Corning 7-59 and 4 mm Chance HA3 filters, providing a transmittance peak around 370 nm. For the green light stimulated luminescence of both quartz and feldspar a similar arrangement was used but of green LEDs, type TLMP 7513 manufactured by III-V, with a maximum in their emission spectrum at 565 nm and providing about 0.2 mW cm^{-2} at the sample. In this case the filters used were Schott 0.5 mm BG39, 4 mm UG 11, Corning 4 mm 7-59, 4 mm 7-60 and Chance 4 mm HA3 which provided a sharper transmittance peak at 360 nm.

Quartz

Preliminary measurements with the green LED system on quartz samples showed that the samples zeroed by heating to 500 °C had a much greater sensitivity to the beta dose than the samples zeroed in the solar stimulator, table 1. Because of this substantial difference in behaviour bleaching tests were carried out on samples zeroed in both ways. The percentage reduction in OSL intensity is plotted against duration of light exposure in fig.1 which however shows no distinction between method of zeroing despite the difference in sensitivity. Fig. 1 does show that there is a marked dependence of rate bleaching on the colour of the light even when allowance is made for the different intensities from the three colours of fluorescent tube used, as noted above. That comparison of the red and gold light data indicates greater bleaching for a given energy absorbed by the sample as the wavelength is reduced suggests that the short wavelength components in the white light are responsible for its rapid bleaching. The reduction in bleaching effect with increasing wavelength in fig. 1 is similar to the wavelength dependence of the bleaching of the 325 °C thermoluminescence peak in quartz reported by Spooner *et al.* (1988).

Feldspar

The sensitivity of the feldspar samples as measured with the green LEDs was less dependent on the method of zeroing than in the case of quartz, table 1, the heated feldspar being only about 30% more sensitive than the optically zeroed feldspar. Nevertheless for completeness bleaching tests were carried out on samples zeroed in both ways, with the results displayed in fig. 2. As was the case with quartz, the rate of bleaching is not significantly dependent on the method of zeroing. However in marked contrast to the quartz results the energy required form the bleaching light to produce a particular reduction in OSL intensity is not significantly dependent on the colour of the light.

Similar measurements were made on the bleaching of the infra red stimulated luminescence of feldspar samples, fig. 3. In this case the material zeroed by heating showed about 40% greater sensitivity than the optically zeroed material although again the method of zeroing did not influence the rate of bleaching. As with the green OSL, the degree of bleaching is not obviously dependent on the colour of the bleaching light but only on the energy absorbed. Indeed the dependence of degree of bleaching on energy from the fluorescent light is essentially the same in figs. 2 and 3, i.e. for both green and infra red stimulated luminescence from feldspar.

Conclusions

While the bleaching of green OSL from quartz is dependent on the colour of the light, the bleaching of both green and infra red OSL from feldspar is essentially similarly dependent on the energy absorbed from the bleaching light independent of colour over the visible range. As a guide to a maximum acceptable exposure of samples to light, table 2 lists the energy per unit area which produces a 1% bleaching of OSL. Also listed is the time required for a 40 W 1200 mm long red, gold or white tube at a distance of 1 m from the sample to produce 1% bleaching. Except for quartz exposed to red light, the times are all very short. For feldspar the longer times for gold and red light simply relate to the lower light intensity from the coloured fluorescent tubes rather than to the colour as such. In so far as the same light sensitive traps in the sample crystals may be relevant to both OSL and recently described thermoluminescence techniques for the dating of sediments, Franklin and Hornyak (1990), Prescott and Fox (1990), the limitations of table 2 may apply also to sediment samples for such thermoluminescence dating, even though the TL signal is generally considerably less sensitive to light than the OSL signal from the same material (Godfrey-Smith et al, 1988).

Acknowledgements

It is a pleasure to thank Mr H J Napier for his invaluable assistance with this work.

References

Franklin, A. D. and Hornyak, W. F. (1990) Isolation of the rapidly bleaching peak in quartz TL glow curves. *Ancient TL* **8**, 29-31.

Galloway, R. B. (1991) A versatile 40-sample system for TL and OSL measurement. *Nucl. Tracks and Radiat. Meas.* **18**, 265-271.

Galloway, R. B. and Napier, H. J. (1991) Alternative laboratory illumination: 'gold' fluorescent tubes. *Ancient TL* **9**, 6-9.

Godfrey-Smith, D. I., Huntley, D. J.. and Chen, W. H. (1988) Optical dating studies of quartz and feldspar sediment extracts. *Quat. Sci. Rev.* **7**, 373-380.

Prescott, J. R. and Fox, P. J. (1990) Dating quartz sediments using the 325 °C TL peak: new spectral data. *Ancient TL* **8**, 32-34.

Spooner, N. A., Prescott, J. R. and Hutton, J. T. (1988) The effect of illumination wavelength on the bleaching of the thermoluminescence (TL) of quartz. *Quat. Sci. Rev.* **7**, 325-329.

Thorn EMI Lighting (1987) *The Comprehensive Catalogue 1987/88*, pp. 209, 216, 217.

PR Reviewed by D. Godfrey-Smith

Table 1.
Relative OSL intensity for samples of comparable mass and given the same beta dose (240 Gy) and pre-heat (60s at 200°C).

sample zeroing	quartz SOL-2	feldspar SOL-2	feldspar 500 °C	quartz 500 °C
rel.int.	1	29	37	77

Table 2.
Best estimate from the data of the energy per unit area and exposure times for a 1 % reduction in OSL intensity. The exposure times refer to a 40 W 1200 mm fluorescent tube at a distance of 1 m from the sample.

fluorescent light colour	Green LEDs quartz J m^{-2}		 feldspar J m^{-2}		Infra red LEDs feldspar J m^{-2}	
red	350	5 Hrs	7	6 min	10	8 min
gold	60	10 min	7	1 min	10	2 min
white	5	10 s	7	15 s	10	20 s

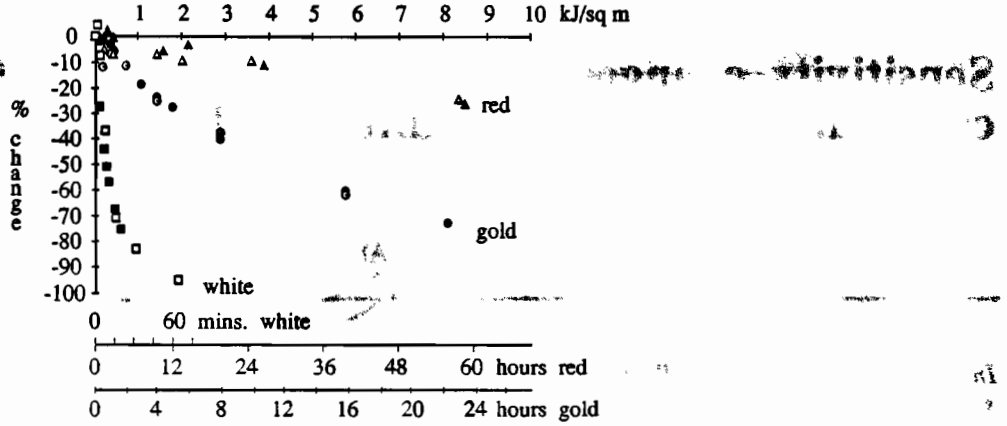

Figure 1. The dependence of the percentage reduction in green LED stimulated luminescence from quartz on the energy per unit area delivered by the fluorescent tubes to the sample (upper axis, based on the manufacturer's data and duration of exposure). The corresponding duration of exposure to white, red and gold fluorescent tubes (40 W 1200 mm long) at a distance of 1 m is given on the lower axes. The solid symbols refer to samples zeroed by heating to 500 °C and the open symbols to optically zeroed samples.

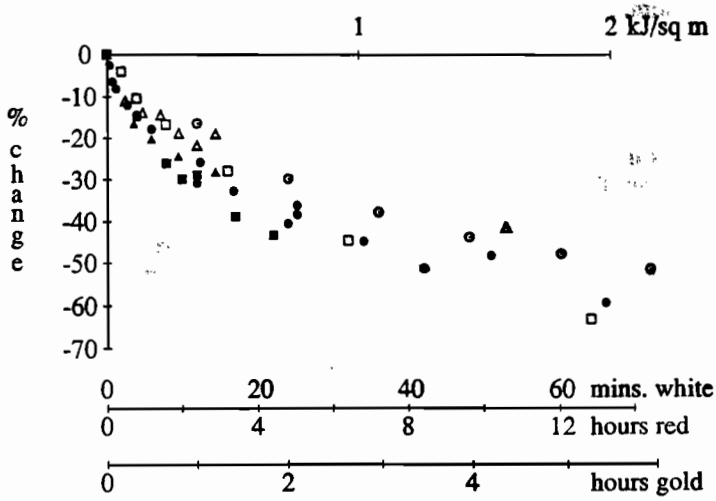

Figure 2. Data on the bleaching of feldspar luminescence stimulated by green LEDs in the same format as figure 1. Squares refer to white light, triangles to red light and circles to gold light, solid symbols to samples zeroed by heating to 500°C and open symbols to samples optically zeroed.

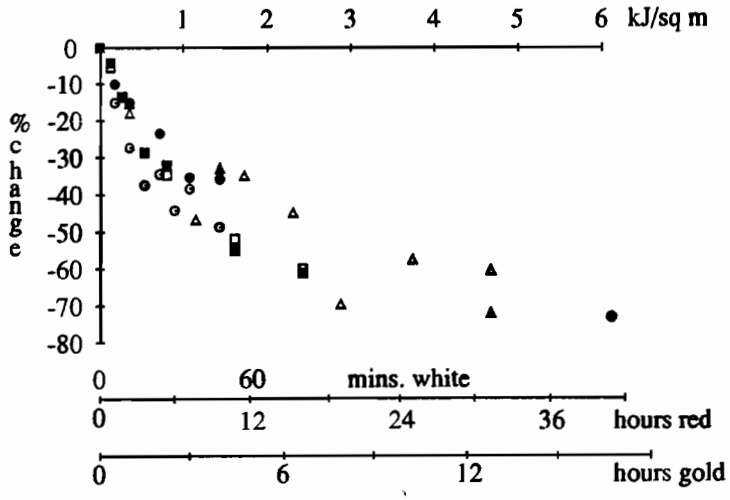

Figure 3. Data on the bleaching of feldspar luminescence stimulated by infra red LEDs in the same format as the previous figures.

Sensitivity changes of luminescence signals from colluvial sediments after different bleaching procedures

Sheng-Hua Li and A.G. Wintle
Institute of Earth Studies, University College of Wales, Aberystwyth SY23 3DB. U.K.

In a luminescence study of colluvial sediment samples we compared the Equivalent Doses (EDs) obtained by infrared stimulated luminescence (IRSL) and by thermoluminescence (TL) on the identical sample discs. For the youngest sample the IRSL ED was considerably smaller than the ED obtained by TL, thus demonstrating the advantage of this methodology. For the older samples there was a similar overestimation (about 60 Gy) of the ED by TL.
During this study the sensitivity of the IRSL signal was observed after bleaching with a solar simulator and with infrared radiation. The experiments suggested that the sensitivity change is related to the degree of sunlight exposure prior to deposition.

Introduction

In optical dating methods the stimulated luminescence signals are bleached quickly by sunlight (Huntley et al., 1985). It has been suggested that these methods can be used to date materials which have not received prolonged sunlight exposure prior to deposition. For such materials optical dating methods might be expected to have a considerable advantage over TL methods where the residual signal must be considered. In this study we set out to demonstrate this advantage by looking at colluvial deposits from Natal, South Africa (Botha et al. 1990). These sheet wash deposits lie on a low slope and transport distances from source are of the order of 1 km. Previous TL results indicate zeroing problems (Wintle et al. 1992).

Considerable thought has been given to the possibility of TL sensitivity changes induced in the laboratory by artificial light sources and experiments have been carried out using such light sources and sunlight (Wintle 1985). A sensitivity increase has also been reported for the optically stimulated luminescence (OSL) signal from quartz when measured with an argon ion laser (Rhodes, 1990; Smith et al., 1990). Such sensitivity changes would result in incorrect EDs being obtained when using the regeneration method for TL or OSL.

In this paper we examine the implications of sensitivity changes resulting from different illumination histories. The results of IRSL measurements on colluvial deposits after different laboratory light exposures are used to draw conclusions about the effects of the natural light exposure on subsequent ED determinations.

Samples and experimental details

Four colluvial samples (AF-1, AF-2, AF-3 and AF-4) were collected from the St.Paul section at Nqutu, Kwa Zulu, South Africa. Fine grains 4-11 μm were deposited on Al discs using routine preparation methods and were split into four groups for ED determination by additive dose and regeneration methods. Different bleaching treatments were applied to three of the groups prior to using the regeneration method to obtain the ED (a) infrared bleaching for 1600 seconds by the Risø IR/TL system (Bøtter-Jensen et al. 1991). The infrared power at the disc is about 40 mW cm^{-2}. (b) bleaching for 1600 seconds by a Honle SOL2 solar simulator. (c) bleaching for 15 hours by the Honle SOL2. After each bleaching treatment, the IRSL had been reduced to a negligible level, close to the background level measured for a blank disc.

Irradiation was performed with a Daybreak irradiator. To remove the unstable component in the IRSL signal, preheating for 16 hours at 140 °C was performed for all discs and there was at least 24 hours delay after irradiation and after preheating. The IRSL measurements were carried out using an infrared LED array mounted above a Daybreak TL oven. The LEDs were TEMT 484 and the power on the sample disc was about 20 mW cm^{-2} for a current of 20 mA. The IR wavelength (880 ± 80 nm) used for stimulation was the same as that used for the IR bleaching in the Risø IR/TL system. The only optical filter in front of the EMI 9635QB photo-multiplier tube was a 2 mm thick Schott BG 39. The data was taken with an Ortec ACE-MCS card. An integrated photon count for 0.1 seconds (within a 0.12 second exposure) was used, which gives a negligible reduction of the TL signal after each measurement. Subsequent TL measurements were carried out in the Riso reader with two optical filters, one Corning 7-59 and one HA3, in front of the EMI 9635QB photomultiplier tube. The heating rate was 5 °C s^{-1} up to 450 °C.

Growth curves were constructed for both regeneration and additive dose methods. Because the IRSL response was not linear for the three older samples, an exponential curve fitting programme developed for TL growth curves (Smith, 1983) was used.

Results

Typical IRSL growth curves obtained after the different bleaching procedures are shown in fig ure 1a. Each data point represents the mean of 4 measurements. The initial slope (X_o) of the growth curve represents the sensitivity of IRSL after bleaching, and was calculated with the parameters from the fitting curves. For

$$IRSL = k - a\exp(-bD)$$

D is the dose. k, a and b are the fitting parameters.

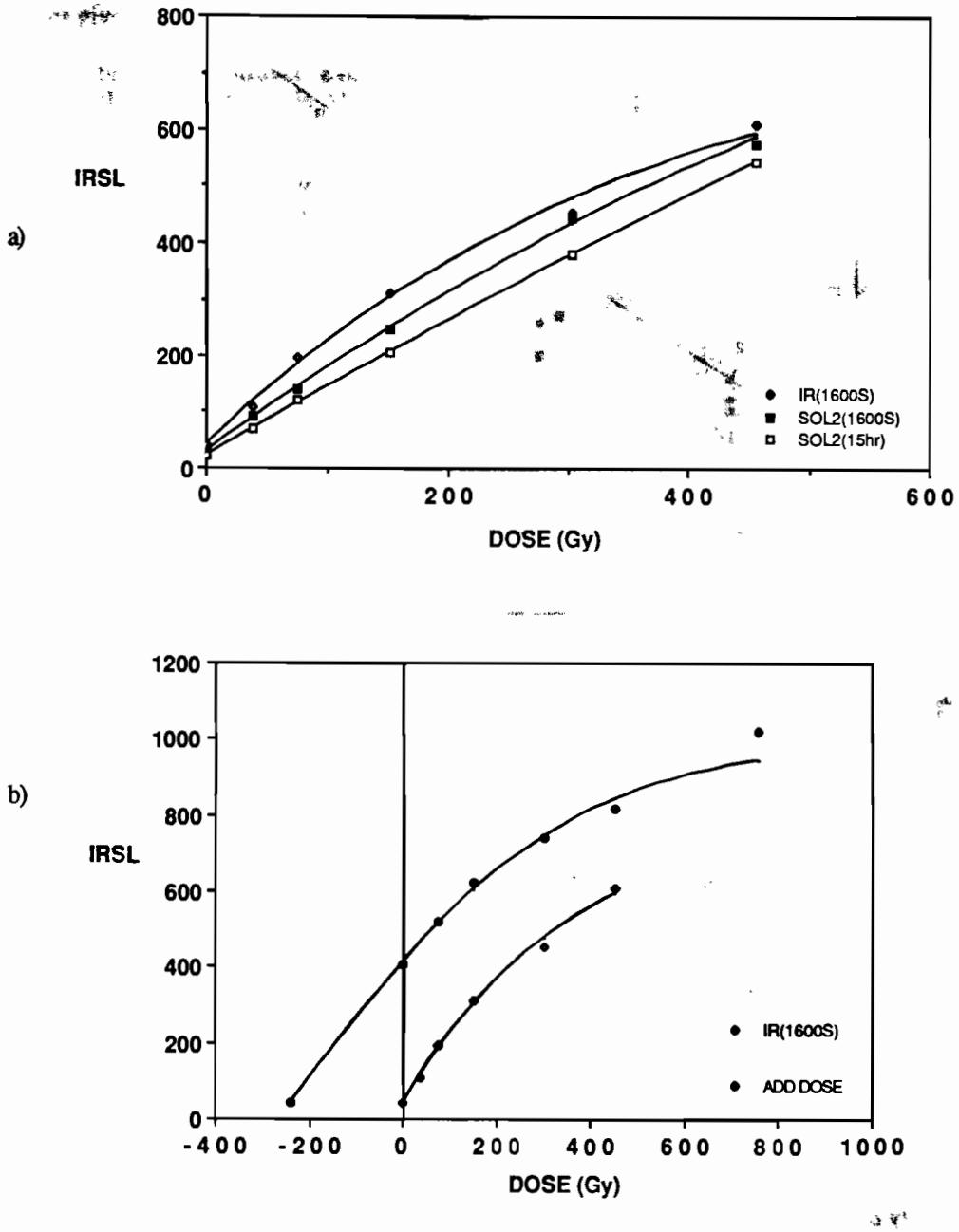

Figure 1. Growth curves for sample AF-1. a) Regeneration after exposure to IR and SOL2. b) additive dose and regeneration after IR bleaching.

The initial slopes were given by

$$X_o = ab \exp(-bED) \text{ and } X_o = ab \ (ED=0)$$

for the additive dose method and the regeneration method respectively. The results are summarised in fig ure 2a in which the sensitivity for the additive dose method is plotted against the sensitivity after bleaching for the three different treatments.

Discussion

The sensitivity of the IRSL signal for the 3 oldest samples decreases with bleaching time when using the SOL2 solar simulator. A short bleach (1600 s) with IR gives a higher sensitivity than for either SOL2 bleach (figs. 1a and 2a). Significantly different EDs for the regeneration method were thus obtained using these bleaching procedures (table 1 and fig. 2b). In each case the IRSL was bleached to a negligible level before regeneration, and hence the ED differences cannot be explained by the presence of different residual levels.

A comparison of the regenerated IRSL ED values with those given by the additive dose method for the remaining group of discs suggests that only the ED determined after IR bleaching is apparently similar to the additive dose ED for all four samples (fig. 2b; table 1).

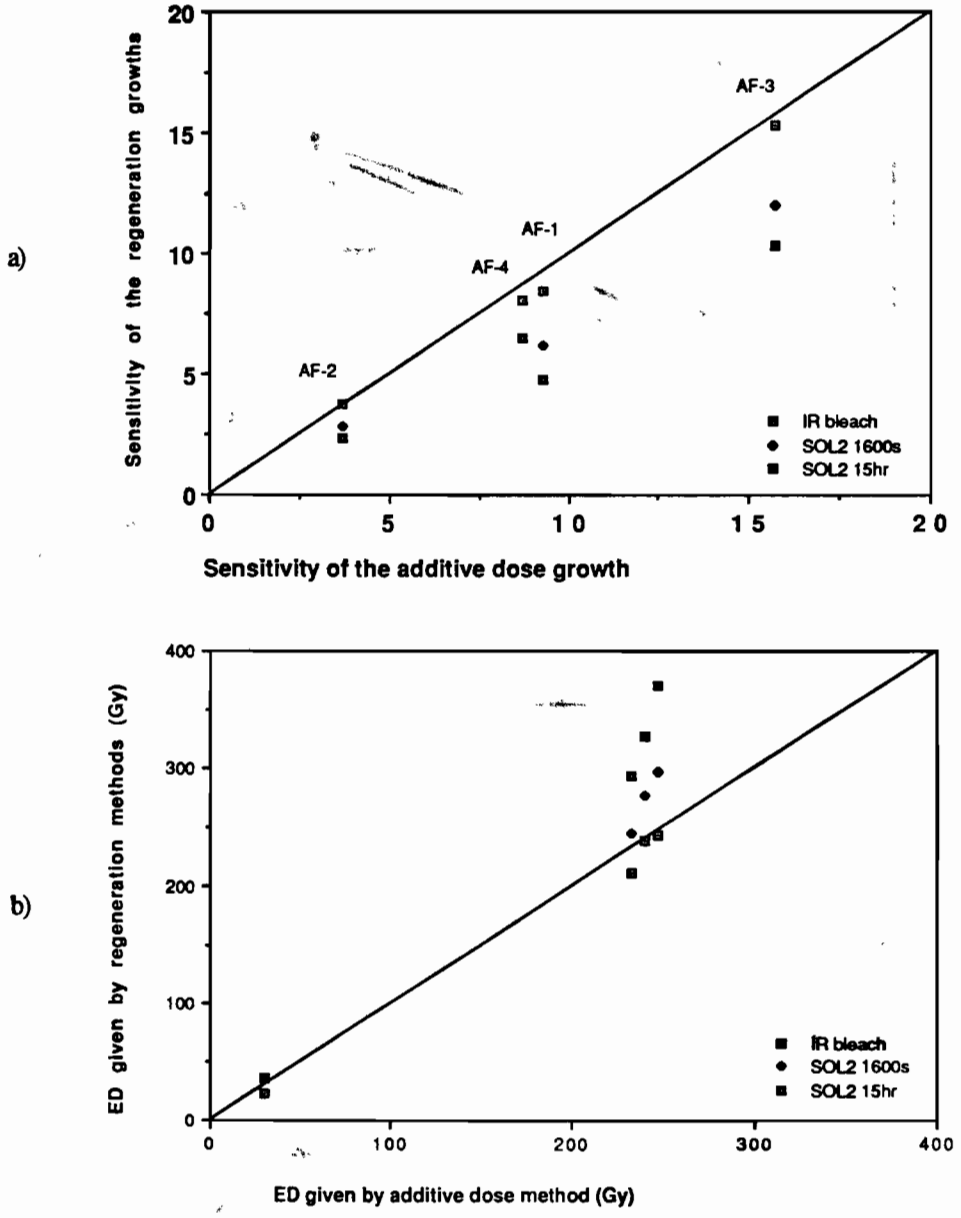

Figure 2. a) Sensitivity of initial IRSL signal measured after bleaching versus the initial sensitivity as obtained by extrapolation for the additive growth data sets. b) IRSL EDs obtained by the regeneration method using different bleachings versus that obtained by the additive dose method for 4 colluvial sediments. The line has a slope of 1.

Table 1. Equivalent dose given by IRSL and TL methods

method		samples AF-4	AF-3	AF-2	AF-1
ADD.Dose	IRSL ED	30 ± 1	233 ± 10	248 ± 21	240 ± 22
	TL ED	90 ± 3	264 ± 15	319 ±14	424 ± 53
Regen. (IR bleach)	IRSL ED	23 ± 3	212 ± 6	243 ± 23	238 ± 23
Regen.	IRSL ED	-	245 ± 14	297 ± 25	277 ± 23
(SOL2 1600s)	TL ED	-	218 ± 3	291 ± 36	295 ± 30
Regen.	IRSL ED	35 ± 4	293 ± 11	371 ± 32	328 ± 23
(SOL2 1600s)	TL ED	104 ± 1	342 ± 20	453 ± 53	451 ± 42

Note. TL residual after 15 hours SOL2 bleaching was used in the ED calculation of the additive dose method.

The ED values given by routine TL measurement were higher than those given by any of the IRSL measurements (table 1). This difference is most clearly demonstrated for the youngest sample AF-4, for which the TL ED was 3 times larger than the IRSL ED. The age derived from the IRSL additive dose ED (5.2 ± 0.3 ka) still gives an overestimate when compared with the ^{14}C date (1.5 ka) from an underlying soil horizon. In spite of this discrepancy the IRSL method is more appropriate for these colluvial samples than TL.

Previous studies on aeolian sediments suggest that the sensitivity of TL signals (Wintle 1985; Rendell and Townsend, 1988) and OSL signals (Smith et al., 1990) changes after laboratory bleaching, with the sensitivity increase being negligible for young samples but significant for old samples (Zhou and Wintle, 1989). These findings contrast with those observed in this study since the IRSL sensitivity decreased rather than increased after bleaching with the SOL2. Not only was this decrease in sensitivity found in older samples, but also in the young sample AF-4. The general difference between aeolian and colluvial sediments is the degree of sunlight exposure prior to deposition. Given the results of the above bleaching experiments, it is possible that the nature of the exposure before deposition could alter the post-depositional IRSL sensitivity of the sample.

Conclusions

The choice of bleaching time and wavelengths to reduce the IRSL signal to a negligible level affects the subsequent response to laboratory dose. This would lead to significantly different EDs being obtained. Comparison of the additive dose ED and EDs obtained by regeneration, suggests that IR bleaching should be used for methods using the regeneration concept, including a single disc approach. That laboratory light exposures can affect IRSL sensitivity suggests that the extent of light exposure prior to incorporation in a sediment deposit will have an effect on subsequent ED determinations. This is confirmed by measurements which show that the decrease in sensitivity of the IRSL signal after SOL2 bleaching found for colluvial samples is not found for loess (Li and Wintle, in preparation).

Acknowledgements

We would like to thank Dr. B.W. Smith for the use of his exponential fitting programme, G.A. Botha of the Geological Survey of South Africa for providing the samples, and F.M. Musson and G.A.T. Duller for stimulating discussions. SHL is partially supported by the Great Britain-China Educational Trust and has a studentship from the Institute of Earth Studies, U.C.W. IRSL research is funded by a NERC grant GR9/333 to AGW.

References

Botha, G.A., De Villiers, J.M. and Vogel, J.C. (1990) Cyclicity of erosion, colluvial sedimentation and palaeosol formation in Quaternary hillslop deposits from northern Natal, South Africa. *Palaeoecology of Africa* **21** , 195-210.

Botter-Jensen, L., Ditlefsen, C. and Mejdahl, V., (1991) Combined OSL (infrared) and TL studies of feldspars, *Nuclear. Tracks and Radiat. Meas.* **18** , 257-263.

Li, S-H. and Wintle, A.G. Sensitivity change due to bleaching of sediments. (in preparation).

Huntley, D.J., Godfrey-Smith, D.I. and Thewalt, M.L.W. (1985). Optical dating of sediments. *Nature* **313**, 105-107.

Rendell, H.M. and Townsend, P.D, (1988) Thermoluminescence dating of a 10 m loess profile in Pakistan. *Quaternary Science Reviews* **7**, 251-255.

Rhodes, E.J., (1990), Optical dating of quartz from sediments. Unpublished D.Phil. thesis, University of Oxford.

Smith, B.W., (1983) New applications of thermoluminescence dating and comparisons with other methods, Unpublished Ph.D. thesis, University of Adelaide.

Smith, B.W., Rhodes, E.J., Stokes, S., Spooner, N.A. and Aitken, M.J. (1990) Optical dating of sediments: initial quartz results from Oxford. *Archaeometry* **32**, 19-31.

Wintle, A.G., (1985) Sensitization of TL signal by exposure to light. *Ancient TL* **3**, 16-21.

Wintle, A.G., Li, S-H. and Botha, G.A. (1992) Luminescence dating of colluvial deposits. Proceedings of the 10th SASQUA biennial conference, Port Elizabeth (in press).

Zhou, L-P. and Wintle, A.G. (1989), Underestimation of regeneration ED encountered in Chinese loess, in *Synopses from a workshop on long and short range limits in luminescence dating*, Oxford, April 1989, Res. Lab. Archaeol. Hist. Art, Oxford. University, occasional publication, 9.

PR Helen Rendell

Bibliography

Batchelor, J. D. and Sears, D. W. G. (1991) Metamorphism of eucrite meteorites studied quantitatively using induced thermoluminescence. *Nature* **349**, 516-518.

Berger, G. W., Burke, R. M., Carver, G. A. and Easterbrook, D. J. (1991) Test of thermoluminescence dating with coastal sediments from northern California. *Chemical Geology* (Isotope Geoscience Section) **87**, 21-37.

Forman, S. L. (1991) Late Pleistocene chronology of loess deposition near Luochaun, China. *Quaternary Research* **36**, 19-28.

Fragoulis, D. V. and Readhead, M. L. (1991) Feldspar inclusions and the anomalous fading and enhancement of thermoluminescence in quartz grains. *Nuclear Tracks and Radiation Measurements* **18**, 291-296.

Grün, R. and Stringer, C. B (1991) Electron Spin Resonance dating and the evolution of modern humans. *Archaeometry* **33**, 153-199.

Ikeda, S., Kasuya, M. and Ikeya, M. (1991) ESR ages of Middle Pleistocene corals from the Ryukyu Islands. *Quaternary Research* **36**, 61-71.

Mercier, N., Valladas, H., Joron, J-L., Leveque, F. and Vandermeersch, B. (1991) Thermoluminescence dating of the late Neanderthal remains from Saint-Cesaire. *Nature*, **351**, 737-739.

Murray-Wallace, C. V. and Goede, A. (1991) Aminostratigraphy and electron spin resonance studies of late Quaternary sea level change and coastal neotectonics in Tasmania, Autralia. *Zeitschrift für Geomorphologie* **35**, 129-149.

Nambi, K. S. V., Iyer, M. R., Bhatt, B. C., Srivasata, J. K. and Patil, A. S. (1990) Dating of an alpha-contaminated TLD badge. *Bulletin of Radiation Protection* **13**, 25-27.

Nanson, G. C., Price, D. M., Short, S. A., Young, R. W. and Jones, B. G. (1991) Comparative uranium-thorium and thermoluminescence dating of weathered Quaternary alluvium in the tropics of Northern Australia. *Quaternary Research* **35**, 347-366.

Page, K. J., Nanson, G. C. and Price, D. M. (1991) Thermoluminescence chronology of late Quaternary deposition on the riverine plain of south-eastern Australia. *Australian Geographer* **22**, 14-23.

Prescott, J. R., Akber, R. A. and Gartia, R. K. (1990) Three-dimensional thermoluminescence spectroscopy of minerals. Chapter 10, Spectroscopic Characterization of Minerals and their Surfaces (eds L. M. Coyne, S. W. S. McKeever and D. F. Blake), *ACS Series* **415**, 180-189.

Rendell, H. M. (1989) Loess deposition during the Late Pleistocene in Northern Pakistan. *Zeitschrift fur Geomorphologie* **76**, 247-255.

Rendell, H. M., Gardner, R. A. M., Agrawal, D. P. and Juyal, N. (1989) Chronology and stratigraphy of Kashmir loess. *Zeitschrift für Geomorphologie* **76**, 213-223.

Roberts, R. G., Jones, R. and Smith, R. G. (1990) Thermoluminescence dating of a 50,000 year old human occupation site in northern Australia. *Nature* **345**, 153-156.

Zöller, L. and Wagner, G. A. (1990) Thermoluminescence dating of loess recent developments. *Quaternary International* **7/8**, 119-128.

TL dates in

Kolstrup, E. and Houmark-Nielsen, M. (1991) Weichselian palaeoenvironments at Kobblegard, Mon, Denmark. *Boreas* **20**, 169-182.

Lonne, I. and Mangerud, J. (1991) An Early or Middle Weichselian sequence of proglacial, shallow marine sediments on western Svalbard. *Boreas* **20**, 85-104.

Volume 34 of Radiation Protection Dosimetry contained several papers of direct relevance to dating and are listed below.

Aitken, M. J. (1990) TLD methods in archaeometry, geology and sediment studies. *Radiation Protection Dosimetry* **34**, 55-60

Copty-Wergles, K., Nowotny, R. and Hille, P. (1990) Lyoluminescence of calcium carbonate and possible applications in the dating of loess and soils. *Radiation Protection Dosimetry* **34**, 79-82.

Fragoulis, D. and Stoebe, T. G. (1990) Relationship of anomalous fading to feldspar inclusions in quartz. *Radiation Protection Dosimetry* **34**, 65-68.

Hütt, G. and Jaek, I. V. (1990) Photoluminescence dating on the alkali feldspars: Physical backgound, equipment and some results. *Radiation Protection Dosimetry* **34**, 73-73.

Kirsch, Y., Kristianpoller, N. and Shoval, S. (1990) Kinetic analysis of natural and beta-induced TL in albite. *Radiation Protection Dosimetry* **34**, 63-66.

Smith, B. W., Rhodes, E. J., Stokes, S. and Spooner, N. A. (1990) The optical dating of sediments using quartz. *Radiation Protection Dosimetry* **34**, 75-78.

Spooner, N. A., Aitken, M. J., Smith, B. W., Franks, M. and McElroy, C. (1990) Archaeological dating by infrared-stimulated luminescence using a diode array. *Radiation Protection Dosimetry* **34**, 75-78.

Wallner, G., Wild, E., Aref-Azar,. Hille, P. and Schmidt, W. F. O. (1990) Dating of Australian loess deposits. *Radiation Protection Dosimetry* **34**, 69-72.

Yang, X. H. and Mckeever, S. W. S. (1990) Point defects and the pre-dose effect in quart. *Radiation Protection Dosimetry* **34**, 27-30.

Titles of abstracts relating to luminescence or ESR dating presented at the XII INQUA Congress held in China in August 1991

Agrawal, D. P. A Review of Quanternary palaeoclimatic research in Kashmir, India.
Berger, G. W., Pillans, B., Davis, J. O., Palmer, A. and Busacca, A. Tephrochronometry using thermoluminescence of glass and associated loess.
Balescu, S. and Lamothe, M. Thermoluminescence dating of Pleistocene raised beaches from Europe.
Boenigk, W. and Frechen, M. Chronostratigraphy of eolian sediments from Germany and its palaeoclimatic application.
Botha, G. A., Wintle, A. G. and Vogel, J. C. Late Quaternary palaeosols and cyclical landscape development of northern Natal, South Africa.
Bruckner, H. Sea level changes since 300,000 BP as documented in tectonically mobile (Mediterranean) and stable (India) zones.
Deng, J. X. ESR dating for loess-like rocks in Changchun area and its geological interpretation.
Dijkmans, J. W. A. Comparative thermoluminescence and optically stimulated luminescence dating studies using late Pleistocene eolian and fluvial sands and silts from the Netherlands.
Duller, G. A. T. Luminescence dating of Pleistocene raised marine terraces, southern North Island, New Zealand.
Frechen, M. Systematic TL dating of loess profiles from Germany.
Grün, R. Contribution of ESR dating to the reconstruction of modern human evolution.
Baolin, H., Cai, X. C. and Zheng, H. H. ESR age of fossil lamprotula from Dingcun section.
Huang, P. H. et al Study of ESR dating on Peking-man site.
Lamothe, M. and Marcheterre, B. Thermoluminescence of fine grains in till and its potential for dating glacial sediments.
Lazarenko, A. A., Semenov, V. V. and Penkov, A. V. Excursions of geomagnetic field during the Brunhes epoch in loess formation of Central Asia and their stratigraphical significance.
Lees, B. G., Lu, Y. C. and Price, D. M. Reconnaissance thermoluminescence dating of dunes at Cape St Lambert, east Kimberleys, north-western Australia.
Li, S. H., Aitken, M. J. and Zhang, Z. H. Optical dating of loess: potential and problems.
Lu, L. C., Huang, B. L. and Zheng, H. H. An application of TL chronology to late Pleistocene environmental studies.
Lu, Y. C. et al A preliminary geochronology of the climate stratigraphy in northern China since about 150 ka BP.
Malaeva, E. V. and Kulikov, O. A. Late Pleistocene pollen floras from the dated loess sequences of Kopetdag (Turkmenia).
Molodkov, A. and Raukas, A. ESR dating of Quaternary mollusc shells and its use for solving main stratigrpahical problems.
Nie, G. Z. Study of ESR dating with Al center of quartz in Chinese loess.
Pecsi, M. and Zöller, L. Loess chronology and TL dating.
Rhodes, E. J. Optical dating of Quaternary sediments.
Shi, J. S. TL dating; its limitation and stratigraphical meaning of loess.
Singhvi, A. K., Bronger, A., Heinkiele, T. and Someswhar Rao, M. Chronology of climatic change based on loess-palaeosol sequences in central Europe, Indian and China.
Stokes, S., Gaylord, D. R. and Jaworowski, C. Quartz optical dating of selected aeolian sediments from the west-central and northwestern United States.
Wintle, A. G. Luminescence dating techniques.
Xie, J. and Aitken, M. J. Fading and luminescence dating.
Xie, J. and Aitken, M. J. U-series disequilibrium in Chinese loess; the implication to TL, ESR and optical dating.
Xie, J. and Aitken, M. J. Optical dating: new concept for loess by Ar^+ laser.
Zhang, J. Z. and Lu, Y. C. Study on residual TL of the coarse grain and fine grain quartz in the aeolian deposits.
Zheng, G. W. Thermoluminescence dating of stalagmite from Shihua cave.
Zhou, L. P. and Wintle, A. G. Dating Chinese loess by thermoluminescence.
Zöller, L. and Pecsi, M. Thermoluminescence dating of middle and east European loess.

Compiled by Ann Wintle

Notices

° *Change of address*

From January 1992, Dr. Rainer Grün's address will be:

Radiocarbon Research Unit
Australian National University
GPO Box 4
Canberra 2601
Australia.

° *Photomultiplier tubes*

Nigel Spooner has written to *Ancient TL* on behalf of the Research Laboratory for Archaeology, Oxford, regarding the availability of photomultiplier tubes surplus to their requirements. The available quantities and types are:

1, EMI 6255; 1, EMI 9594 QB; 2, EMI 6256

The only charge payable is for postage of the PMT. Interested laboratories should write to Nigel Spooner at:
The Research Laboratory for Archaeology, 6 Keble Road Oxford OX1 3QJ.
tel. 0865 -515211 Fax. 0865-273932.

° *Conferences*

REMINDER

10th Solid State Dosimetry Conference

Georgetown University Conference Centre, Washington D.C., July 13-17 1992

Those requiring details of the conference should contact without delay:
Dr SWS McKeever
Department of Physics
Oklahoma State University
Stillwater
OK 74078, USA
tel. USA-405-744-5802
fax. USA-405-744-7673

(The deadline for abstracts was 15 November.)

Ancient TL SUPPLEMENT

Date List

November 1991 Issue 5

1. This list includes dates for fired materials of archaeological interest, submitted to *Ancient TL* during 1991 for which sufficient information has been supplied. Readers are referred to earlier issues of the Date List for a fuller description of the structure of entries.

2. Application forms are available from the Editor, who will be pleased to advise on data compilation; laboratories wishing to submit dates for which the current date entry specification is not suitable should write to him. The application forms may be supplied on either paper or magnetic media.

Laboratory: [*name*] **Date Entry Specification** **Entry:** [*entry number*]

PART I

Site: [*Name*] **Location:** [*Region, country*] **Grid Ref.:** [*National map reference*]

Site Description: [*Brief description of period and nature of site*]

Dates/Ages:

			Lab. Ref.	Material	Archaeological Ref.
[*Type*] Context / Single	[*Type*] Date / Age	[*Lab. abbrev.*]			
TL		**800 AD ± 50 (Dur87TLfg)**	**100-1/6**	**pottery**	**ABC-1a**

[*Overall error*] [*Test year*] [*Technique*] [*Sample ref.*] [*Dated material*] [*Context reference*]

— **TL Context Components:** [*Details of component TL dates/ages used to derive Context Date/Age*] —

Archaeological Evidence: [*Excavator's brief description of context(s)*]

Site Director: [*Full name and institutional postal address*]

Reports: [*Details of excavation and laboratory reports*]

PART II

Section A. TL Measurements

1. **min.**([*mineral*]) **tech.**([*technique*]; [*grain size range, gsr*] μm)

Data tabulated for each sample:

2. **P** = [*value*] ± s.e. Gy 2a. **I/P** = [*value*] 3. **Slopes** [2nd/1st: [*value*] ± s.e.]
4. [*Type of plateau*] **Plateau** [± [*value*] %; [T_1 - T_2]]
4a. **Peak** [@ [*value*] °C ; [*heating rate*]°/s; [*pre-heat details if applicable*]]
5. **Stability**[[*interval*, T_1 - T_2]; [*period*]; [*storage T* °C]; [*result* ; [*value*] ± [*value*]%]]
6. *a* value = [*value*] or *b* value = [*value*]

Section B. Dose-rate Measurements

Data tabulated for each sample:

1. **Total Effective Dose-rate** = [*value*] ± s.e. mGy/a [α = [*value*]% [*method*]; ß = [*value*]% [*method*]; γ = [*value*] % [*method*]; cos(mic) = [*value*] % [*method*]]
2. **Radon** [± [*value*] % [*method*]]
3. **Water** [Sample ([*value*] ± s.e. %); (Burial) Environment ([*value*] ± s.e. %)]

Section C. Error [[*Procedure : eA76 or specify other*]]

Section D. TL Age

Data tabulated for each sample:
TL Age[± [*random error*]; ± [*overall accuracy*]]

Special Remarks: [*Details of entries with * or any other additional information*]

KEY TO ABBREVIATIONS

STANDARD METHODS/TECHNIQUES/PROCEDURES

i	Inclusion	pd	Pre-dose	*a* Plat	Age plateau
fg	Fine-grain	MA	Multiple activation	*d* Plat	Dose plateau
mmi	Multi-mineral	ADD	Additive dose proc.	*s* Plat	TL Signal plateau
		Sb	Sensitivity baseline		
α-c	Alpha counting	FPh	Flame Photometry	TLD	TL dosimetry
AAS	Atomic absorption	NAA	Neutron Activation Analysis	XRF	X-ray fluorescence
β-c	Beta counting	PXE	PIXIE		
CAP	Capsule	SPEC	Spectrometer (SpEC = portable)		
Non-standard	AutoR	Auto regeneration		PTTL	Photo-transferred TL

MINERALS & ETC.

cal	Calcite	Nf	Sodium feldspar	*	Other
ft	Flint	p	Polymineral	-	Not applicable
f	Feldspar	q	Quartz	e	Equivalent to (used as prefix)
Af	Unsep. alkali feldspar	z	Zircon		
Kf	Potassium feldspar	por	Porcelain	a	Year

Terms: I, P, *a* , *b*, A, S_N, S_o, TAC: as defined in the literature.

Laboratory: Oxford **Entry: 46**

Site: Beedenbostel
Location: Near to Celle, Lower Saxony. Topographic Map 3327 Beedenbostel, Germany.
Grid Ref.: R 3585648.97, H 5834271.65

Site Description: This is an "open air "site, with several pre- and protohistoric occupations, from the late Upper Palaeolithic and Mesolithic onwards.

Dates				Lab. Ref.	Mat'l	Archaeological Reference
TL single dates:	2.80	; ± 0.30 ka	(Ox90TLi)	268a2	burnt quartz	34, 53/51
	3.10	; ± 0.30 ka	(Ox90TLi)	268a3	"	94, 53/51
	8.65	; ± 0.78 ka	(Ox90TLi)	268b4	"	188, 54/50
	3.10	; ± 0.30 ka	(Ox90TLi)	268c5	"	102, 57/51
	9.88	; ± 0.78 ka	(Ox90TLfg)	268c11	burnt flint	113, 54/52

Archaeological Evidence: Two of the younger dates(268a2,268a3) correspond to the late Bronze Age.They are acceptable for dating structure No.1 , a sort of hearth not dateable by archaeological means.

Site Director: Dr. S. Veil, Oberkustos, Niedersachsisches Landesmuseum, Am Maschpark 5, 3000 Hannover 1, Federal Republic of Germany.

Reports: In preparation.

Laboratory: Oxford **Entry: 46**

PART II
TECHNICAL SPECIFICATION

Section A. TL Measurements

1. Mins (Burnt quartzes and burnt flint) tech.(qi and fti (90 - 125 μm), fg(1 - 8 μm)

Sample Ref.	P ± s.e. (Gy)	I/P	Slps	s Plateau	Peak	Stability	a val.
268a2	12.65 ± 0.65	0	0.85 ± 0.05	± 3%; 350-400°	375°; 5°/s;	-	
268a3	7.70 ± 0.40	0	1.08 ± 0.05	± 3%; 325-375°	350°; 5°/s;	-	
268b4	6.05 ± 0.30	0	1.20 ± 0.05	± 3%; 300-450°	300°; 5°/s;	-	
268c5	12.90 ± 0.60	0	0.80 ± 0.05	± 3%; 300-400°	375°; 5°/s;	-	
268c11	5.70 ± 0.30	0	-	± 5%; 325-375°	375°; 5°/s;	325- 375°; 0.5 a; 18°;100 ±3%	0.07

Section B. Dose-rate Measurements

Sample Ref.	Total Eff. Dose-rate	Dose-rate Components α	β	γ	cos.	Radon	Water Sample	Env.
	mGy/a	%	%	%	%	%	%	%
268a2	4.55 ± 0.70	-	91	6	3	0 ± 10	0 ± 2	24 ± 6
268a3	2.49 ± 0.39	-	84	11	5	"	"	"
268b4	0.70 ± 0.10	-	41	41	18	"	"	"
268c5	4.17 ± 0.62	-	90	7	3	"	"	"
268c11	0.58 ± 0.08	8	20	49	23	"	"	"
Method		α-c	α-c FPh	SPEC	SpEC	α-c SPEC		

Section C. Error [eA76]

Section D. TL Age

Sample Ref.	TL Age ka	Errors Random ka	Overall ka.
268a2	2.80	-	0.30
268a3	3.10	-	0.30
268b4	8.65	-	0.78
268c5	3.10	-	0.30
268c11	9.88	-	0.78

Copyright © 1991 *Ancient TL Supplement* Date List ISSN 0735-1348
Date List entries may be reproduced on the understanding that the source is acknowledged

Laboratory: Oxford **Entry:** 47

Site: Els Colls
Location: Tarragona, Spain
Grid Ref.: 41°.17'.10".N., 0°.45'.20".E.
Site Description: The site is a rock shelter in the Sierra de Monsant area of Tarragona. The flints are from the burnt soil horizon at the base of level two.

Dates			Lab. Ref.	Mat'l	Archaeological Reference
TL Context Age:	13.0 ; ±1 ka	(Ox90TLfg)	270f	burnt flint	e2, 10B
TL single ages:	11.6 ; ±1 ka	"	270f1	"	89/2733
	12.7 ; ±1.2 ka	"	270f2	"	88/1488
	11.2 ; ±1 ka	"	270f3	"	88/519
	10.8 ; ±1 ka	"	270f4	"	89/1745
	19.3 ; ±2 ka	"	270f5	"	88/1589
	12.1 ; ±1.1 ka	"	270f6	"	89/2647
	11.7 ; ±1 ka	"	270f8	"	89/5319
	16.1 ; ±1.6 ka	"	270f9	"	89/2790

Archaeological Evidence: The flints are from level 2, which contains fire-places and a lithic industry of Upper Palaeolithic type. Level 4 is of the same typology. First indications placed the site around 20 to 25 ka BP, but the TL age fits well with the C-14 dates of other sites with similar lithic industries.

Site Director: Prof. Dr. J. Ma. Fullola i Pericot,University of Barcelona, Dept. of Prehistory and Archaeology, Baidiri Reixac, 08028 Barcelona, Spain.

Reports: None published.

Laboratory: Oxford **Entry:** 47

PART II
TECHNICAL SPECIFICATION

Section A. TL Measurements

1. Min (burnt flint) tech.(fg ; 1 - 8 μm)

Sample Ref.	P ± s.e. (Gy)	I/P	Slps	s Plateau	Peak	Stability	a val.
270f1	51.5 ± 1.5	0	-	± 5%; 300-400°	375°; 5°/s;	300 - 400°; 0.5 a; 18°; 100 ± 3%	0.125
270f2	60.2 ± 3	"	-	± 2%; 350-450°	"	350 - 450°; "	0.146
270f3	55.6 ± 2.6	"	-	± 5%; 350-450°	"	350 - 450°; "	0.09
270f4	65 ± 2.5	"	-	± 3%; 325-400°	"	325 - 400°; "	0.10
270f5	39 ± 2	"	-	± 3%; 325-400°	"	325 - 400°; "	0.052
270f6	46.2 ± 2.6	"	-	± 5%; 350-400°	"	350 - 400°; "	0.058
270f8	59.9 ± 1.8	"	-	± 2%; 350-400°	"	350 - 400°; "	0.103
270f9	88 ± 4	"	-	± 3%; 350-450°	"	350 - 450°; "	0.074

Section B. Dose-rate Measurements

Sample Ref.	Total Eff. Dose-rate	Dose-rate Components α	β	γ	cos.	Radon	Water Sample	Env.
	mGy/a	%	%	%	%	%	%	%
270f1	4.43 ± 0.65	59	34	6	1	0 ± 5	0 ± 2	4 ± 4
270f2	4.73 ± 0.70	66	27	6	1	"	"	"
270f3	4.94 ± 0.74	56	38	5	1	"	"	"
270f4	5.99 ± 0.90	59	36	4	1	"	"	"
270f5	2.02 ± 0.30	39	46	13	2	"	"	"
270f6	3.83 ± 0.57	45	47	7	1	"	"	"
270f8	5.10 ± 0.77	59	35	5	1	"	"	"
270f9	5.45 ± 0.82	52	42	5	1	"	"	"
Method		α-c	α-c FPh	CAP SPEC	SpEC	α-c SPEC		

Section C. Error [eA76]

Section D. TL Age

Sample Ref.	TL Age ka	Errors Random ka	Overall ka.
270f1	11.6	-	1
270f2	12.7	-	1.2
270f3	11.2	-	1
270f4	10.8	-	1
270f5	19.3	-	2
270f6	12.1	-	1.1
270f8	11.7	-	1
270f9	16.1	-	1.6

Copyright © 1991 *Ancient TL Supplement* Date List ISSN 0735-1348
Date List entries may be reproduced on the understanding that the source is acknowledged

Laboratory: Oxford **Entry:** 48

Site: Little Hoyle Cave
Location: Penally, Dyfed,Wales, England
Grid Ref.: -
Site Description: Limestone cave in a small side valley off the river valley.

Dates			Lab. Ref.	Mat'l	Archaeological Reference
TL Single Date:	9430 ; ±800 a	(Ox90TLfg)	273f	flint	L. H. 90: NP 1049

Archaeological Evidence: The burnt flint was a small blade core of "Mesolithic" type stratified in the latest phase of a succession of screes. These are presumed largely Late Glacial age and are overlying probable loess, overlying frost shattered bedrock.

Site Director: Dr. H. Stephen Green, Keeper of Archaeology and Numismatics, National Museum of Wales, Cathays Park, Cardiff, CF13NP.

Reports: Green, H.S. (1986) The Palaeolithic Settlement of Wales Research Project: A Review of Progress 1978-1985. in *The Palaeolithic of Britain and it's nearest neighbours: Recent Trends* (Ed. S. N. Collcutt) Recent Trends Series, Vol.1. Published by Dept. of Archaeology and Prehistory, University of Sheffield. ISBN 906090 27X.

Laboratory: Oxford **Entry:** 48

PART II
TECHNICAL SPECIFICATION

Section A. TL Measurements

I. Min. (Burnt flint) tech. (fg; 1 - 8 μm)

Sample Ref.	P ± s.e. (Gy)	I/P	SIps	s Plateau	Peak	Stability	a val.
273 f	5.94 ± 0.28	0	-	± 3%; 350-400°	375°; 5°/s;	350 - 400°; 0.3 a; 18°; 100 ± 3%	0.184

Section B. Dose-rate Measurements

Sample Ref.	Total Eff. Dose-rate	Dose-rate Components α	β	γ	cos.	Radon	Water Sample	Env.
	mGy/a	%	%	%	%	%	%	%
273f	0.63 ± 0.09	19	19	42	20	0 ± 5	0 ± 2	10 ± 5
Method		α-c	α-c FPh	CAP SPEC	SpEC	α-c SPEC		

Section C. Error [eA76]

Section D. TL Age

Sample Ref.	TL Age a	Errors Random a	Overall a.
273f	9430	-	800

Copyright © 1991 *Ancient TL Supplement* Date List ISSN 0735-1348
Date List entries may be reproduced on the understanding that the source is acknowledged

Laboratory: Oxford **Entry:** 49

Site: Bossington
Location: The site is in the valley bottom of the river Test at Houghton, Stockbridge, Hants., England.
Grid Ref.: SU 337308
Site Description: Burnt flints are on a mineral palaeosol surface, associated with flint blades. Underneath the overlay is peat with wood, in turn overlain by tufa.

Dates			Lab. Ref.	Mat'l	Archaeological Reference
TL single dates:	7590 ; ±700 a	(Ox90TLfg)	274f1	burnt flint	Site B,Trench 3
	7150 ; ±700 a	"	274f2	"	"
	8700 ; ±850 a	"	274f3	"	"
	7480 ; ±700 a	"	274f5	"	"

Archaeological Evidence: A late Mesolithic date equates with the associated flint blades.There is an adjacent late Mesolithic site of about 4000 flints, but it is less well stratified than the burnt flint.

Site Director: Dr John G. Evans, University of Wales, Dept of Archaeology, PO Box 909, Cardiff CF13XU, UK.

Reports: None published

Laboratory: Oxford **Entry:** 49

PART II
TECHNICAL SPECIFICATION

Section A. TL Measurements

1. Min (flint) tech.(fg ; 1 - 8 μm)

Sample Ref.	P ± s.e. (Gy)	I/P	Slps	s Plateau	Peak	Stability	a val.
274f2	5.65 ± 0.17	0	-	± 2%; 375-450°	375°; 5°/s;	375 - 450°; 0.25 a; 18°; 100 ± 3%	0.088
274f3	8.30 ± 0.46	0	-	± 5%; 350-425°	375°; 5°/s;	350 - 425°; "	0.147
274f5	6.60 ± 0.40	0	-	± 3%; 350-400°	375°; 5°/s;	350 - 400°; "	0.155
274f1	6.98 ± 0.28	0	-	± 3%; 325-400°	375°; 5°/s;	325 - 400°; "	0.187

Section B. Dose-rate Measurements

Sample Ref.	Total Eff. Dose-rate	Dose-rate Components α	β	γ	cos.	Radon	Water Sample	Env.
	mGy/a	%	%	%	%	%	%	%
274f1	0.92 ± 0.14	17	15	54	14	0 ± 5	0 ± 2	60 ± 20
274f2	0.79 ± 0.12	7	13	63	16	"	"	"
274f3	0.95 ± 0.14	17	16	53	14	"	"	"
274f5	0.88 ± 0.13	14	14	57	15	"	"	"
Method		α-c	α-c FPh	CAP SPEC	SpEC	α-c SPEC		

Section C. Error [eA76]

Section D. TL Age

Sample Ref.	TL Age a	Errors Random a	Overall a.
274f1	7590	-	700
274f2	7150	-	700
274f3	8700	-	850
274f5	7480	-	700

Copyright © 1991 *Ancient TL Supplement* Date List ISSN 0735-1348
Date List entries may be reproduced on the understanding that the source is acknowledged